MSc Thesis in Civil Engineering

Verification of multi-axial damage in Glass Fibre-Reinforced Polymer laminates by progressive failure analysis for Civil Engineering applications

Junaid Ahmed

July 2023

A thesis submitted to the Delft University of Technology in partial fulfillment of the requirements for the degree of Master of Science in Structural Engineering

TU Delft

Royal HaskoningDHV
Enhancing Society Together

Verification of multi-axial damage in Glass Fibre-Reinforced Polymer laminates by progressive failure analysis for Civil Engineering applications

by

Junaid Ahmed

To obtain the degree of Master of Science
at the Delft University of Technology,
to be defended publicly on 07.07.2023

Student number: 5393469

Project duration: March 2022 – Juli, 2023

Thesis Committee:	Dr. Marko Pavlovic	TU Delft, Chair of the Committee
	Dr. Fred Veer	TU Delft, supervisor
	Dr. Olena Karpenko	TU Delft, supervisor
	ir. Mathieu Koetsier	TU Delft, supervisor
	ir. Angeliki Christoforidou	TU Delft, supervisor
	ir. Liesbeth Tromp	Royal Haskoning DHV, supervisor

An electronic version of the thesis is available at: ...

Abstract

The use of Glass Fibre-Reinforced Polymer as a building material in structures or structural components is on the rise. Standards such as CUR96, DNV and JRC provide a basis of design with the material. However, there is a lack of confidence in the design phase with structures made of Glass Fibre-Reinforced Polymer, resulting in the use of large safety factors causing the components to be bloated in size. At the time of writing this report, the technical committee, CEN/TC 250 (responsible for developing structural Eurocodes), establishes a technical design specification for Fibre-Reinforced Polymer (FRP) structures. This technical specification describes a simplified and linear criterion to determine the capacity of a GFPR Laminate, in addition to being open for the use of Progressive Failure Analysis (PFA). However, the simplified and linear criterion is overly conservative, whereas there is a lack of faith in the use of the PFA considering the failure theories and degradation models that are currently in use. This report discusses the PFA, a non-linear, 5-step, advanced 2D analysis model, that can predict the static strength of in-plane stress dominated Glass Fibre-Reinforced Polymer laminate, with an arbitrary lay-up composition, based on existing knowledge and experiments, including the damage development under multi-axial stress states and stress redistribution. The research is limited to in-plane behavior, under tensile and compressive stresses. The static material response is characterized on a unidirectional ply level based on principal directions and based on experimental results obtained from the OptiDat program. The response predicted by the PFA for both tension and compression was in reasonable agreement with the experimental results. However, depending on the failure theory and degradation model used, there is potential for optimistic predictions of the laminate stress capacity. For future work, it is recommended to continue the research on a larger variety of laminate lay-ups and include more failure theories and degradation models.

Keywords:

(a) Glass fibre-reinforced polymer
(b) Progressive failure analysis
(c) Static strength prediction

Preface

Dear reader,

The ability to combine different materials with one another to produce a material with properties suitable for various uses has been fundamental to the advancement of human civil engineering. Through my Master's thesis, "Verification of multi-axial damage in Glass Fibre-Reinforced Polymer laminates by progressive failure analysis for Civil Engineering applications", I have taken a small but significant step towards understanding material behavior and exploring its potential as a structural component. Additionally, this thesis marks the culmination of my journey at Delft University of Technology.

I am deeply grateful for the support and collaboration I received from leading experts within the field of FRP during this journey. I would like to express my gratitude to the following individuals, from my committee, who have provided me with invaluable assistance. First and foremost, I want to thank Marko Pavlovic for dedicating his time, guidance, and patience throughout the course of this thesis. I am also grateful to Liesbeth Tromp for sharing her knowledge and keeping me critically aware of my work at each step of the journey. Mathieu Koetsier, for consistently supporting me whenever I encountered obstacles I struggled to solve. Angeliki Christoforidou, for her unwavering support and provision of all the necessary information. Olena Karpenka, for her endless encouragement in the last stage of finishing the thesis. Lastly, I would like to acknowledge Fred Veer for our friendly and insightful discussions on complex matters.

Throughout this thesis, I have acquired a substantial amount of knowledge regarding the behavior of GFRP laminates. Although my research question does not have a straightforward answer, it affirms that I pursued my research in the right area of expertise and made a meaningful contribution to future research.

Junaid Ahmed

Delft, Juli 2023

Contents

Abstract v

Preface vii

Contents ix

List of Tables xii

List of Figures xvi

Glossary xviii

1 Introduction 1

1.1 Project motivation 1

1.2 Problem statement 2

1.3 Goal and Scope 3

1.4 Research Question 4

1.5 Aim and objectives 6

1.6 Research method 7

2 Literature review 8

2.1 Static behavior of GFRP 8

2.1.1 Types of damage 8

2.2 Static life modelling approaches 10

2.2.1 Progressive damage models 10

2.3 Loading the laminate 11

2.3.1 Uni-axial loading 11

2.3.2 Biaxial loading 11

2.4 OptiMat blades project 13

2.5 Assessment according to Code 14

Progressive failure analysis according to Eurocode proposal TS19101 14

2.6 Models of degradation 15

2.7 Failure theories 16

3 Methodology 17
3.1 The design processes 19
3.2 Progressive failure analysis 21
3.3 Experimental input requirements 22
3.4 The cases considered 23
3.5 Failure theories 25
3.5.1 Tsai Wu 25
3.5.2 Hashin 26
3.5.3 Tsai Hill 27
3.6 Degradation models 28
3.7 Limitations in assessment of failure 29
4 Unidirectional laminate under UD loading 31
4.1 On-axis coupons 31
4.2 Off-axis coupons 36
4.3 The angle ply 39
4.4 Review of the method 41
4.5 Conclusion 44
5 Multidirectional laminate under UD loading 45
5.1 Multidirectional laminate under tension 45
5.2 Multidirectional laminate under compression 52
5.3 MD2 under transverse loading 55
5.4 MD2 – Off-axis specimen 58
5.5 Review of the method 62
5.6 Conclusion 66
6 Multidirectional laminate under biaxial loading 67
6.1 Introduction to cruciform specimen 67
6.2 1/0 and 0/1 loading 70

6.3 Irregularities with cruciform experiments 72
6.4 Bi-axial loading ratios 75
6.5 Conclusion 82
7 Conclusions and recommendations 83
7.1 Conclusions 83
7.2 Recommendations 85
References 1
Appendix I 4
Appendix II: Predictions, detailed results 5

List of Tables

Table 3-1: Required static material properties for a PFA 22
Table 3-2: Overview of unidirectional experiments performed as part of the Optimat project23
Table 3-3: Overview of multidirectional experiments performed as part of the Optimat project 23
Table 3-4: Overview of bi-axial experiments performed as part of the Optimat project..... 24
Table 3-5: Reduction of material properties in case of matrix failure of ply 28
Table 4-1: Overview of unidirectional experiments carried out during the OPTIMAT project 31
Table 4-2: Summary of experiments on unidirectional coupons during the OPTIMAT project 32
Table 4-3: Comparison of experimental and Tsai Wu predictions on unidirectional coupons 32
Table 4-4: Summary of predictions on on-axis experiment 33
Table 4-5: Comparison of UD off-axis experimental results and prediction with Tsai Wu and Total Discount 36
Table 4-6: Overview of predictions of off-axis coupons, all numbers in N/mm^2 37
Table 4-7: PFA predictions with Tsai Wu and Total Discount compared with the experimental result 39
Table 4-8: Summary of the predictions for 45s-T laminate 40
Table 4-9: Update of prediction of 45s-T with failure indices applied to Tsai Wu and Tsai Hill criteria..... 42
Table 5-1: Summary of mean geometrical properties of tensile and compressive MD coupons used in experiments 45
Table 5-2: Summary of mean experimental results from tensile and compressive tests 46
Table 5-3: Experimental results and PFA prediction, comparison of initial and final failure . 46
Table 5-4: Summary of predictions on MD2 specimen compared to experimental result..... 47
Table 5-5: Inaccuracy of each prediction compared to experimental result on MD2 specimen 48
Table 5-6: Improvement that can be achieved if failure theories are combined with the Residual Property model 49
Table 5-7: Prediction of failure with Tsai Wu and Total Discount..... 52
Table 5-8: Summary of predictions on MD2 specimen under compression compared to experiment..... 53

Table 5-9: Summary of prediction on MD2 under compression compared to experiment in percentage 53
Table 5-10: Summary of MD2 on-axis experimental results 55
Table 5-11: MD transverse specimen predictions, compared to experiments 56
Table 5-12: MD transverse specimen predictions in percent difference, compared to experiments, negative are optimistic 56
Table 5-13: Overview of geometrical properties of MD2 off-axis beamlike coupons 58
Table 5-14: Overview of experimental results of MD2 off-axis beamlike coupons 58
Table 5-15: Summary of MD off-axis predictions compared to the experiment 59
Table 5-16: Summary of MD off-axis predictions compared to experimental results, in percentages 60
Table 5-17: Statistical characterization of experimental results on MD2 laminate 62
Table 5-18: Proposed model factors to be applied to predictions with Residual Discount 64
Table 6-1: Overview of biaxial experiments performed as part of OptiDat scope 68
Table 6-2: Overview of experimental results on cruciform specimen subject to biaxial loading 69
Table 6-3: Comparison of unidirectionally loaded MD2 specimen as beamlike and cruciform specimen 70
Table 6-4 Summary of predictions on unidirectionally loaded biaxial coupons 70
Table 6-5: MD2 cruciform subject to tensile load, in percentage inaccuracy 71
Table 6-6: Comparison of stress and strain of unidirectionally loaded biaxial coupon 72
Table 6-7: Summary of predictions with PFA on the Cruciform specimen with main loading ratio in the Y-direction 75
Table 6-8: Summary of predictions on Cruciform specimen with main loading ratio in the Y-direction, in percentage 76
Table 6-9: Summary of PFA predictions on cruciform specimen with main loading ratio in x-direction 76
Table 6-10: Summary of PFA predictions on cruciform specimen with main loading ratio in the x-direction, in percentages 77
Table 6-11: Standard deviation and 95% confidence interval for the cruciform specimen, all loading ratios 79
Table 7-1: Summary of in-plane mechanical properties from OPTIMAT UD material based on experimental results in GPa ..... **Feil! Bokmerke er ikke definert.**

Table 7-2: Summary of in-plane mechanical strength properties from OPTIMAT UD material based on ecperimental results..... **Feil! Bokmerke er ikke definert.**
Table 7-3: Overview of initial and final failure predictions with Tsai Wu combined with degradation models ..... **Feil! Bokmerke er ikke definert.**
Table 7-4: Overview of initial and final failure predictions with Hashin combined with degradation models ..... **Feil! Bokmerke er ikke definert.**

Table A-I 1Summary of in-plane mechanical properties from OPTIMAT UD material based on experimental results in GPA 4
Table A-I 2: Summary of in-plane mechanical strength properties from OPTIMAT UD material based on experimental results in GPA 4

Table A-II a: Summary of experiment on UD on-axis specimen compared to predictions..... 5
Table A-II b 10-T laminate, detailed predictions with Tsai Wu 6
Table A-II c 10-T laminate, detailed predictions with Tsai Hill..... 6
Table A-II d 10-T laminate, detailed predictions with Hashin..... 7
Table A-II e 10-C laminate, detailed predictions with Tsai Wu 7
Table A-II f 10-C laminate, detailed predictions with Tsai Hill 7
Table A-II g 10-C laminate, detailed predictions with Hashin 8
Table A-II h 60-T laminate, detailed predictions with Tsai Wu 9
Table A-II i 60-T laminate, detailed predictions with Tsai Hill..... 9
Table A-II j 60-T laminate, detailed predictions with Hashin 9
Table A-II k 60-C laminate, detailed predictions with Tsai Wu..... 11
Table A-II l 60-C laminate, detailed predictions with Tsai Hill 11
Table A-II m 60-C laminate, detailed predictions with Hashin 11
Table A-II n 0-MDC laminate, detailed predictions with Tsai Wu..... 13
Table A-II o 0-MDC laminate, detailed predictions with Tsai Hill..... 13
Table A-II p 0-MDC laminate, detailed predictions with Hashin..... 13
Table A-II q 0-MDT laminate, detailed predictions with Tsai Wu..... 14
Table A-II r 0-MDT laminate, detailed predictions with Tsai Hill..... 14
Table A-II s 0-MDT laminate, detailed predictions with Hashin..... 14
Table A-II t 60-MDT laminate, detailed predictions with Tsai Wu..... 16
Table A-II u 60-MDT laminate, detailed predictions with Tsai Hill 16

Table A-II v 60-MDT laminate, detailed predictions with Hashin 17
Table A-II w 10-MDT laminate, detailed predictions with Tsai Wu 18
Table A-II x10-MDT laminate, detailed predictions with Tsai Hill 18
Table A-II y 10-MDT laminate, detailed predictions with Hashin 18
Table A-II z 10-MDC laminate, detailed predictions with Tsai Wu 20
Table A-II aa 10-MDC laminate, detailed predictions with Tsai Hill 20
Table A-II bb 10-MDC laminate, detailed predictions with Hashin 20

List of Figures

Figure 2-1: Damage progression in GFRP laminate as the applied stress is increased 8
Figure 3-1: Reference system to be used for the thesis, x- and y-direction 18
Figure 4-1: Stress-strain plots of unidirectional coupons under compressive loading. On left: 90-C under compression. On the right: 0-C. 34
Figure 4-2: Stress-strain graph of 90-C laminate under compression. Experiment vs Prediction 35
Figure 4-3: Stress-Strain plots of off-axis coupons, experimental (blue) and predicted (orange) results 36
Figure 4-4 Stress strain graph of the experimental and the predicted result 39
Figure 4-5: Plot of 45s-T specimen, experimental result, and prediction with Hahsin and Residual discount 40
Figure 4-6: MD laminate under tension, prediction vs experiment 42
Figure 5-1: Visualization of PFA prediction and experimental results of MD2 laminate under tension on a stress-strain graph 47
Figure 5-2: PFA of MD2 laminate under tension with Hashin criterion, combined with different degradation models 49
Figure 5-3: 10-MD2 laminate under compression, prediction vs experiment 52
Figure 5-4 0-MDC, experiment vs prediction 54
Figure 5-5: Failure envelope for MD laminate, visualized in the 4 quadrants. The mean value is represented by blue dots, and 95 percentile values are represented by arrows. 63
Figure 5-6: Failure envelopes for Hashin criterion, with color. Green: Total Discount. Red: Residual discount. Blue/black: Mean experimental result 63
Figure 5-7: Stress-strain diagrams for the experimental results, the black line denotes the strain limit 65
Figure 6-1: Geometry of cruciform specimen used in experiments 68
Figure 6-2: Visualization of stress calculations from Guidelines for biaxial testing of FRP using a cruciform specimen 73
Figure 6-3: A comparison of the methods to calculate the stresses in the central area from “Guidelines for biaxial testing of fibre reinforced composites using a cruciform specimen” [16] 74
Figure 6-4: Summary of PFA predictions on cruciform specimen in stress space visualized . 78

Figure 6-5: Plot of lower and upper 95% confidence level for experimental results and predictions with Residual discount, with three black lines representing the upper, mean, and lower bound. 80
Figure 6-6 Experimental results of cruciform specimen in force-space 81

Glossary

Symbols

$E_{1,c}$	Parallel compression stiffness of UD plies
$E_{1,t}$	Parallel tension stiffness of UD plies
E_1	Parallel modulus of UD plies
$E_{2,c}$	Transverse compression stiffness of UD plies
$E_{2,t}$	Transverse tension stiffness of UD plies
E_2	Transverse modulus of UD plies
E_x	Modulus of the laminate in UD plies
E_y	Parallel compression stiffness of UD plies
G_{12}	Shear modulus of UD ply
G_{xy}	Shear modulus of the laminate
V_f	Parallel compression stiffness of UD plies
ν_{12}	Poisson's ratio 12-direction
ν_{21}	Poisson's ratio 21-direction
σ_x	Stress parallel to fibre direction
σ_{11}	Longitudinal stress in a ply
σ_{22}	Transverse stress in a ply
τ_{12}	Shear stress in a ply
PFA	Progressive Failure Analysis
CLT	Classical Laminate Theory
GFRP	Glass Fibre-Reinforced Polymer
FRP	Fibre Reinforced Polymer
FE	Finite Element

UD Unidirectional

MD Multidirectional

UCS Ultimate Compressive Stress

UTS Ultimate Tensile Stress

[Blank page]

1 Introduction

1.1 Project motivation

Composite materials have been used in civilization for a long time. The use of Adobe, a composite material in the form of bricks, can be dated back as far as 5100 B.C. [1]. Since, several materials have been used as building blocks for civilization. The first synthetic polymers were discovered in the later stages of the 19th century and became increasingly popular after the 1950s [2]. For structural applications, glass fibre reinforced polymer (GFRP) is the most widespread polymer composite in use. However, GFRP is still a relatively new material in the civil engineering world, and there is still a lot of work to be done to fully understand the material behavior.

At the current stage, a technical specification is being developed, which can be further advanced into a Eurocode (EC)[3]. The development of a Eurocode for GFRP will make the material more widely known and provide more guidelines and rules when designing FRP structures. It will further boost the research on the material, as well as more experience can be gained from structures where it has been applied. A more thorough understanding of the material will enable designers to design more efficient structures.

1.2 Problem statement

For a consultancy firm, such as Royal HaskoningDHV, efficient design according to a safe procedure is important. To produce an efficient GFRP design for a structure, an in-depth understanding of the material and related failure theories is essential. Therefore, it is desirable to increase the understanding of how the failure of a laminate and related theories can be utilized for an improved design process.

When choosing between methods of verification, it is typical to select the conservative method, thus err while ensuring safety [4]. This uncertainty in design and the judicious use of safety factors leads to excessively expensive and inefficient structures due to increased material usage. This uncertainty is not only related to the material but also to the design process itself. This is apparent in the prediction of final failure of the laminate, which shows a greater lack of accuracy with the usage of failure criteria compared to prediction of initial failure. This is because fibers can carry higher loads than expected after initial failure, and progressive failure is a dynamic process occurring inside the material, this makes it hard to study the deformations and damage accumulation in each layer [5]. This leads to the usage of failure criteria in the initial sizing of the material, thereafter, testing of the material to determine the final design. This is a slow and costly procedure, and there is a desire to increase the utility of failure theories by translating the results into more efficient design procedures.

The understanding of how to incorporate progressive failure leading to final failure into the design process is still limited, leading to inefficient procedure and wasteful use of material in GFRP structures. The experience and maturity of knowledge is not on the level of other commonly used materials in structural applications. Hence, the technical committee, CEN/TC 250, which is responsible for developing Eurocodes, is working on a technical specification for design purposes for FRP structures[3]. For a laminate, the ultimate failure may (“may” indicates an action is permissible within limits of EC) be estimated using “the Classical Laminate Theory” by a 5-step procedure based on ply properties. To predict the failure of a single ply, Tsai-Hill failure criterion and Tsai-Wu failure criterion are outlined, and other failure criteria are only mentioned.

1.3 Goal and Scope

Limitations and boundaries are set to ensure the research is completed in the prescribed amount of time and with high quality. The research in this study will be focused on static loaded in GFRP laminates dominated by in-plane stresses, excluding environmental and temperature effects. This study will make use of existing knowledge found in the literature and existing test results- found in the OptiMat database. Performing experiments is not within the scope of this study.

The Research is limited to the static behavior of the GFRP material and prediction on the component level. Where the behavior of the components can be described mainly by in-plane stresses, out-of-plane, and through-thickness behavior is not considered to be a point of focus. Moreover, considering the failure theories, the thesis will limit itself by not altering the theories in any way as part of the PFA.

1.4 Research Question

The main research question and sub questions are formulated based on the information provided in the problem statement. The main research question is:

"What is the inaccuracy by which the static performance of in-plane dominated Glass Fibre-Reinforced Polymer laminates under multiaxial stress states can be predicted by progressive failure analysis as described in TS19101, based on existing knowledge and experimental results?"

To answer the main research question systematically, three sub research questions have been formulated.

1. *How inaccurate is the method specified in TS19101 Annex B.8 in predicting the final failure of a GFRP laminate under static loading?*

Investigating the performance of a GFRP laminate using PFA, the research aims to assess the predictive capabilities of PFA as outlined in TS19101. The forthcoming Eurocode (TS19101 Annex B.8) presents a five-step process, including the Classical Laminate theory, for analytically predicting the ultimate failure of a laminate. However, Annex B.8 of TS19101 leaves certain steps open-ended in terms of their implementation in PFA. To explore this five-step procedure, a comprehensive literature review will be conducted.

2. *Considering the cause of the inaccuracy exposed in the initial predictions, how can the predictions of progressive failure analysis be improved to better represent laminate behavior?*

The research will compare the initial predictions from subquestion 1 with experimental results to identify the underlying reasons for the inaccuracy. To enhance the understanding of the physical behavior of GFRP laminates and their response to static loading, the study will review pertinent literature on failure theories and degradation models. This investigation is performed to identify improvements in prediction accuracy through the PFA procedure.

3. *What recommendations might be given to engineers considering the time and effort used in making the predictions, compared to the level of accuracy achieved?*

Drawing from the knowledge obtained through subquestion 1 and 2, the third subquestion aims to provide specific recommendations to engineers who want to utilize PFA in the design of structures.

1.5 Aim and objectives

This research aims to understand the GFRP performance under static loading conditions in UD and bi-axial loading directions, to be able to better predict the behavior of GFRP laminates through PFA as described in the TS19101. The following objectives will contribute to the aim of this study:

1. Literature review of the state-of-the-art in static performance of GFRP laminates
    a. Static behavior of GFRP
    b. Failure theories
    c. Degradation models
2. Prediction of failure through PFA, and improvements to the model
    a. Based on the procedure described in the TS19101, predict the last ply failure of GFRP laminates.
    b. Review the procedure after each chapter for interpretations and suggest optimization.

1.6 Research method

Literature is scanned for qualitative and quantitative data to better understand the static behavior of GFRP laminates. The existing knowledge will contribute to building a deeper understanding of the performance of GFRP until final ply failure is reached, including the influence on laminate properties and possible damage mechanisms. Moreover, previous research will provide insight into the effectiveness of failure theories and degradation models in predicting the failure behavior of the GFRP laminates. Additionally, it will highlight the crucial factors that must be considered for more accurate predictions of static performance.

2 Literature review

2.1 Static behavior of GFRP

GFRP is a structural material that demonstrate a high degree of complex behavior when subject to static loading depending on the layup and type of loading. As the load is increased, the plies within the laminate will begin to fail. However, initial failure of the lamina, or ply failure, does not necessarily mean total failure of the structural component. Rather, damage will continue to accumulate in the laminate, ending with the final failure of the laminate. The strength of a GFRP laminate will be reliant on the direction of the fibers and might display anisotropic behavior to a larger extent than comparable materials. Metals are homogeneous and isotropic, whereas GFRP is inhomogeneous and anisotropic. Therefore, the knowledge of steel behavior is not possible to be directly applied to GFRP laminates. Furthermore, variability in material configurations will affect the performance of a laminate depending on fiber type, matrix type, material lay-up, and different manufacturing methods. This variability makes it challenging to develop a commonly accepted procedure to verify the design performance [6].

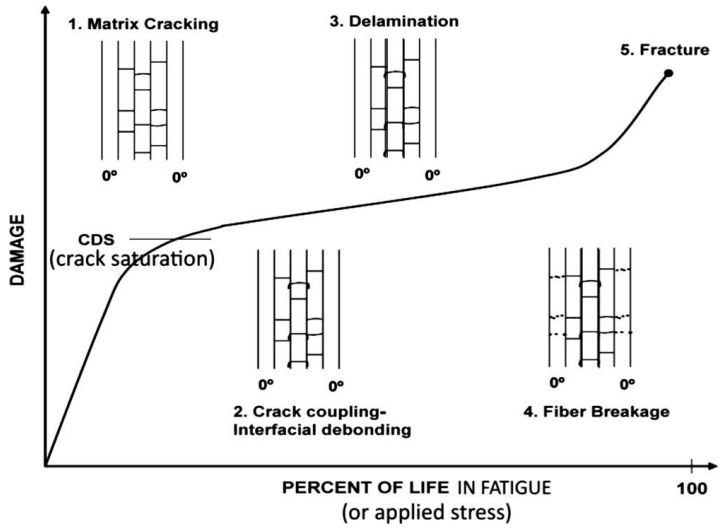

Figure 2-1: Damage progression in GFRP laminate as the applied stress is increased[6]

2.1.1 Types of damage

Multiple types of damage could occur in composites. The occurrence depends on the stress state, the crack initiation, and the propagation energy of the different damage mechanisms and can be described in five stages, see Figure 2-1. Even though Figure 2-1 was developed for fatigue, it can be illustrative of damage accumulated due to static loading as well.

Damage normally starts with the development of cracks within the plies of a laminate perpendicular to the direction of loading, which continues to develop until the characteristic damage state is reached and crack saturation is achieved [7]. The damage initiation, called "intralaminar damage" when within plies, will often occur in regions with lower strength in the laminate, such as in the matrix. With a continued increase of loading the second stage is reached, and the ply cracks will divert into the ply interfaces, called "inter-laminar damage", establishing connections between cracks across the plies. This propagation of cracks will continue to plies with different fibre directions helped by stress concentrations at crack tips. In the third stage, the cracks continue to connect with one another across ply interfaces, leading to the separation of plies, also known as delamination. There are many causes of delamination, one such instance is the result of interlaminar shear stresses caused by intralaminar cracks that reduce the stiffness of a ply considerably compared to adjacent plies. Lastly, fiber breakage is the final stage of damage propagation in the laminate, normally in the fiber direction of which the compressive or tensile loading is applied. Statistical distribution of fibre properties of fibres, can in practice lead to early fiber breakage of the weaker individual fibres, leading to a redistribution of the stresses to surrounding plies. The redistribution of stresses can cause failure in adjacent plies if the stresses are large enough, leading to progressive failure breakage before the final failure of the laminate is reached[4].

It is important to note that different sequences may lead to the same mechanisms of failure and can be discussed at different material levels. To begin with, failure can be considered to happen in either the matrix or in the fibre. On a larger scale, it can happen on the level of an individual ply. Eventually, one can consider the whole laminate to be failing, involving the whole thickness of the structure or laminate. The standard DNV-ST-C501 considers several such sequences of failure [8].

2.2 Static life modelling approaches

The linear-nonlinear response and complex failure mechanisms of failure in multidirectional GFRP laminates make it difficult to accurately predict the progression of damage and failure of the laminate. Such damage includes damage to the matrix, failure of the fibre, debonding of the fiber-matrix, and interface delamination, and can cause considerable loss of stiffness and function in GFRP laminates. The damage initiation if often a local effect [9].

Finite element simulation of composites has been developed at the macro-scale, considering the whole laminate with averaged behavior, the meso-scale, representing each ply as an equivalent homogeneous layer, and micro-length scales, acknowledging individual fiber-matrix interaction. The classical laminate theory and Rule-of-Mixtures forms the basis of the constitutive models [7].

2.2.1 Progressive damage models

Many types of analytical and computational models including micro–macro modeling approach of progressive damage have been established to predict the deformation and reliability of FRP composite materials and structures [10]. FE simulation of FRP composites has been developed at macro-, meso- and micro-length scales. In simulating FRP composite laminates, the macro-scale model considers the laminate with an average behavior while the micro-scale model acknowledges individual fiber-matrix interaction. The meso-scale model represents each UD FRP composite lamina as an equivalent homogeneous layer. In each case, the FE model requires precise geometry, accurate boundary conditions, and a valid constitutive model [11].

In the failure process of the FRP composite, both the constitutive relations and the damage models for the matrix and reinforcement phases are required where the classical laminate theory and Rule-of-Mixture form the basis for the constitutive model. The observed nonlinear deformation preceding fracture can be described using damage-based models such as stress-based failure criteria for matrix cracking and fiber fracture. Interlaminar damage in FRP composite laminates was represented by cohesive damage models [5].

2.3 Loading the laminate

A structure would normally be subject to a combination of loads acting in more than a single direction at one time. Despite this, most experiments are carried out by applying a UD load to the specimen being studied [12]. To gain insight into material failure, failure envelopes can be produced to show stress combinations applied to a material. Points along the X and the Y axis can be easily validated by standard UD tests in tension, compression, and shear. However, the largest part of this envelope consists of biaxial stress states, which would require testing under biaxial stress states to validate. Considering the complexity related to biaxial testing, there is a lack of biaxial test results available, whereas the available test results are performed under conditions that can leave doubt concerning the validity of the results [13]. An experimental investigation should approximate the real-life behavior of materials as much as possible, as well as be tailored for specific applications as it is difficult to account for all the parameters and simulate their effect on material behavior [14].

2.3.1 Uni-axial loading

Due to its anisotropic nature, different loading conditions and lay-up might affect the development of damage in a laminate in various ways, making it important to differentiate between various conditions. Mechanical testing of composites has often been restricted to uniaxially loaded specimens, and the material properties are optimized for the primary load. However, FRP composites are rarely ever loaded in one direction only, which might result in failure due to small secondary loads coinciding with a weakness in the material [15].

2.3.2 Biaxial loading

The main purpose of performing biaxial tests is to validate failure criteria, which is the focus of this research. Moreover, purposes related to fracture mechanics [16] or realistic representation by applying to structures are examples of other uses of biaxial testing. Biaxial loads can be applied on various types of specimens, single load systems like off-axis testing or biaxial flexure testing, or two loading systems like tubular specimens or planar cruciform specimens.

Listing every technique is not within the scope of this thesis, nonetheless, two conditions must be met for a successful biaxial loading test. Firstly, a test zone with uniform biaxial stress distribution should be obtained. Secondly, specimen failure should occur within the test zone [16].

The cruciform specimen is a straightforward and realistic way of inducing a biaxial stress state in a flat material. Some of the drawbacks are the appearance of stress concentrations outside the biaxial testing zone, the calculation of stresses because they are statically indeterminate, and the required sophisticated testing equipment [16].

2.4 OptiMat blades project

The OptiMat blades project was a joint research project by participants from 10 research institutes from 7 European countries and 5 wind turbine manufacturers from 3 European countries. More than 3000 individual tests were carried out on epoxy GFRP coupons, with the main aim of the project to provide accurate design recommendations for the optimized use of materials within wind turbine rotor blades and improved reliability. The intention was to achieve improved design recommendations for the rotor blades in wind turbines so that reliable blades with optimized material use can be designed with lower weight and less waste of material. The research ended with 39 design recommendations [17].

Task group 2 was among others tasked with investigating the blade material under complex stress states, with the goal of generating test results of basic plies and multidirectional laminates for the reference material. This would be used to define and validate multi-axial failure theories in static and to quantify complex stress state effects on blade design by contributing with design recommendations. Furthermore, all relevant 'static' material properties of the reference material at ambient conditions were characterized using a statistically significant sample size [18], [19].

A large number of uniaxial (on- and off-axis) and multi-axial coupon tests (cruciform shape and tubes) were performed to validate failure criteria and assess reliability methods to accurately predict failure probability. At least 25 individual tests per property were performed, to have a statistical description when measuring 19 engineering constants. The standard OB coupon geometry was used in all static and fatigue tests, except for in-plane shear characterization tests which were based on ISO 14129 specimen geometry and test method. The thickness was altered from coupons tested in the fibre direction to those loaded transversely to the fibre direction, because less plies were used. A comparison of test results with respective results derived from ISO coupons and test methods revealed that values for strength and moduli are in very good agreement, except the compressive strength in the fibre direction, where the OPTIMAT specimen has inferior performance due to bending deformation [17].

2.5 Assessment according to Code

The assessments of the failure of a GFRP laminate in the Eurocode proposal prCENTS19101 draft version from 2020-11-04 (hereby TS19101) can be categorized into two general methods, the simplified criterion in chapter 8.2.9 on laminate level, and the PFA in Annex b.8, performed on ply level. The laminate and ply level analysis can be associated with the macro and micro level analysis, respectively.

Progressive failure analysis according to Eurocode proposal TS19101

The technical specification proposes a method on how to perform the PFA to reach the ultimate failure of fiber composites in five main steps. Before doing so, stiffness and strength properties should be predicted using the Classical Laminate theory based on ply properties. The following steps are defined in the TS19101:

Step 1: Calculate stresses and strains in each ply using CLT.
Step 2: Apply an appropriate failure criterion to predict which ply fails first
Step 3: Assign reduced stiffness and strength to the failed ply
Step 4: Recalculate stresses and strains in each of the plies using CLT
Step 5: Recalculate stresses and strains in each of the plies using CLT

Note that the code does not specify which failure criterion to use, nor which degradation model to apply. However, it goes on to propose three alternative methods to account for the degradation of the laminate as a result of the failure of a ply. The proposal for the degradation models is given in the notes:

Model 1: Total Discount method: All failed plies get assigned zero stiffness and strength in all directions
Model 2: Limited discount method: If the lamina fails in matrix material, the transverse and shear strength are reduced to zero, as well as the shear stiffness. If the lamina fails in the fiber material, Total Discount method is applied to the failed ply.
Model 3: Residual property method: The failed lamina gets residual strength and stiffness applied to it.

Furthermore, the code describes two failure criteria that can be used for the purpose of progressive failure in detail, Tsai-Hill and Tsai-Wu. Other criteria such as Maximum Stress, Maximum Strain, Puck, Hashin are proposed as well-established alternatives to the failure criteria described.

2.6 Models of degradation

The composite material is built up by several highly anisotropic lamina, layered in different directions, leading to complex behavior including failure modes, directionality of failure, and interaction of failed and non-failed plies. Furthermore, the initial failure of the composite is not necessarily associated with the ultimate failure, and the rupture of one lamina may be a benign event due to load sharing and constraining effects provided by adjacent laminae. Loads are redistributed from damaged plies to undamaged plies by the material unloading in some fashion throughout the structure until final failure is reached, and no more loads can be sustained. The ultimate failure can be a complex chain of events and laminates can resist substantial damage before reaching such a point. However, it is not so easy to characterize the remaining strength and stiffness, which is complicated by several possible models to choose from.

Considering some of the complex behavior shown by composite laminates, the most used failure theories vary in accuracy when predicting the failure modes, whereas the degradation models provide an unrealistic response to failure. The models required to do this as termed material property degradation models (MDM). These models may, possibly based on the mode of failure, degrade the material properties, either suddenly, to a fraction of the undamaged properties, or gradually, incrementally reducing the material properties as the damage increases. Models of degradation will be restricted to sudden models of degradation.

The Total Discount model completely cuts the residual stiffness and strength after failure and is the model that is applied in case of fiber failure, as it is associated with the ultimate failure of a ply. The limited discount model can be found in both the Eurocode proposal and DNV-ST-C501, showcasing the difference of opinion regarding what to do with the strength properties when reducing the material properties. The TS19101 proposes a reduction of the stiffness and strength properties, whereas the DNV-ST-C501 only considers the stiffness properties to be reduced while keeping the strength intact. The residual stiffness typically depends on empirical observations or a micromechanics model of prediction with several authors proposing models that work well under certain conditions[20]. The DNV standard also recommends a method to determine the residual properties of a material which can be derived based on experimental results [8].

2.7 Failure theories

A study known as the "World-Wide Failure Exercise" gathered experts from across the world in 1991 intending to establish confidence in the current methods for failure predictions. 19 different failure theories were considered, and the performance of the criteria related to the prediction of failure was investigated. One of the key findings was the lack of faith in the available failure criteria. One of the causes for the inability of the failure criteria to predict the failure of composites is that most of the criteria were developed based on criteria in use for isotropic materials, such as Von Mises for steel, which put the research on the wrong path [15]. More details regarding specific failure criteria will follow in relevant chapters.

There is not much available evidence that failure criteria for composites can provide accurate and meaningful prediction of failure, except for under a limited range of conditions. Often, this will lead to a rather conservative design as large safety factors, set to 30 % of the ultimate load carrying capacity, are needed to ensure the predictions do not go into the optimistic range. As such, the failure theories are often limited to be used on the initial "sizing" of components, and experiments are performed on coupons or structural elements to determine global design allowable [21].

3 Methodology

This chapter aims to further delve into the PFA as it is described in the TS19101 to develop a methodology that is to be followed through this research to be consistent. This will include investigating failure theories and degradation models, as they are an essential part of the successful application of the PFA. The PFA does not strictly specify which failure theories or degradation models must be used in a particular situation, it is therefore up to the designer to choose an appropriate failure criterion and degradation model. To determine the optimal alternative, a literature study to determine which failure theories are relevant, and find suitable degradation models that have been successfully applied to simulate ply behavior post-failure is required.

One of the targets of this research is to use the PFA to simulate the laminates response when subjected to static loading to predict the ultimate failure of a laminate, in order to obtain a more economical design. To accomplish the research with the PFA, ply-level data is needed as input values. The data has been obtained through the OptiDat database. Furthermore, the OptiDat database contains multiple experiments on a multidirectional laminate, loaded parallel and perpendicularly to the main fiber direction, in tension and compression. Using the OptiDat database as the basis for the input values for the prediction of failure in multidirectional laminates ensures consistency and relevance of the results obtained in the research.

Simulating the response, the outcome will be used to determine the inaccuracy that is achieved by the use of the PFA in combination with certain failure theories and degradation models. The results will provide increased confidence for a designer following the TS19101 in what his predictions mean concerning real-world application of his design.

A reference system is established regarding the fiber and loading directions for consistency in referencing the laminate. Unless otherwise mentioned, the x-direction will be parallel to the 0-fibers in the 0-degree laminate under tension, regarded as the strong direction, whereas the y-direction will be perpendicular to the 0-degree laminate under tension, regarded as the weak direction, see Figure 3-1.

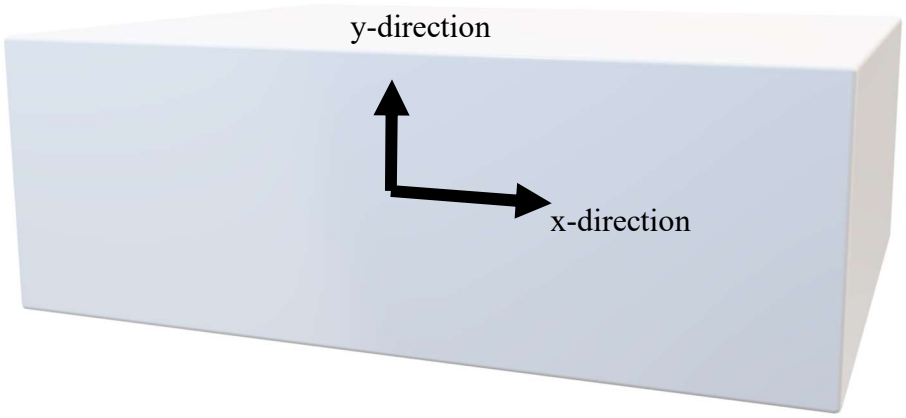

Figure 3-1: Reference system to be used for the thesis, x- and y-direction

3.1 The design processes

Currently, the beginning of a technical specification for fibre-polymer composite structures is prepared by the technical committee CEN/TC 250" Structural Eurocodes". The expectation is that, when the TS19101 is finalized and available, it will become a widely used specification for designing Fibre-Reinforced Polymer (FRP) structures. Therefore, the verification procedure of the TS19101 is used as a framework for the research. Additionally, other design codes, such as DNV-GL-ST-C501, are considered to increase the understanding of how the final failure of a GFRP laminate is understood and implemented in other codes.

A literature study will be conducted into failure theories and degradation models to explore the possibilities provided by the PFA. Building on the information gained in the literature study, a selection of three failure theories and models of degradation for each, are selected to apply the PFA. This is important as the TS19101 does not require the application of any specific failure theory or model of degradation as part of the PFA, rather the designer is free to choose according to his own needs. A study is required to have an initial understanding of the performance and complexity of the failure criteria.

To stepwise build an understanding of the PFA, firstly, the analysis will be applied to the simplest cases, such as the UD laminates under a UD load. The sub research questions will be answered, and based on the results, recommendations will be given regarding the procedure for applying the PFA. Thereafter, the research will move on to the next batch of experimental results representing a more complex case. The chapters will correspond to the complication considered and are summarized as follows:

Chapter 1: Unidirectional laminates subject to unidirectional loading

This chapter will consider the simplest cases in which a tensile or compressive load was applied to a UD laminate. The UD laminates are the same as was used to derive the ply data, therefore, the expectation is that the predictions should be highly accurate. The aim of this chapter is to familiarize with the PFA and is not relevant to be considered in the conclusion chapter for the purpose of this thesis.

Chapter 2: Multidirectional laminates subject to unidirectional loading

The second chapter will consider a multidirectional laminate, named MD2 in the OptiDat database. The MD2 laminate in the OptiDat database, is subject to tensile and compressive UD load in a number of directions which will be outlined at a later stage of this chapter.

Chapter 3: Multidirectional laminates subject to biaxial loading

Lastly, the MD2 laminate will be considered under a range of biaxial loading ratios. The biaxial experiments were carried out on cruciform specimens under tensile loading only. More details about the cruciform specimen geometry will be outlined in the relevant chapter.

3.2 Progressive failure analysis

PFA makes use of the individual ply properties of a laminate and is used to perform an analysis on the ply level. Properties are assigned to each ply in a laminate consisting of a certain thickness and layup. With this information, the CLT can be applied to calculate the ABD matrix of the laminate and obtain the individual ply stresses and strains for any laminate when a load is applied. Subsequently, a failure theory is used to interpret the stresses or strains and predict if failure has occurred [22]. With failure occurring in a ply, a model of degradation can be applied to simulate the post-failure behavior, considering the damaged plies. It is important to understand if an occurring failure is the final failure of the laminate, or if there is residual capacity left for the laminate to carry a higher load. If there is residual capacity, the stresses and strains of the laminate are recalculated with the failed plies, and the analysis can be repeated until final failure is reached. Furthermore, a distinction is made between failure in the matrix and in the fiber in this research, as this will affect the severity of the degradation of the plies.

3.3 Experimental input requirements

All model input requirements are material related. To run a PFA, a complete set of UD data is required, existing static material properties [23]–[25] of the UD ply as outlined in Table 3.1.

Table 3-1: Required static material properties for a PFA

Property	Abbreviation	Standard	Value
Tensile modulus 1-direction	$E_{1,t}$	EN-ISO 527	29 042
Tensile modulus 2-direction	$E_{2,t}$	EN-ISO 527	14 077
Compressive modulus 1-direction	$E_{1,c}$	EN-ISO 14126	
Compressive modulus 2-direction	$E_{2,c}$	EN-ISO 14126	
Shear modulus	G_{12}		4 239
Poisson's ratio 12-direction	ν_{12}		0.291
Tensile strength 1-direction	$S_{1,t}$		776.5
Tensile strength 2-direction	$S_{2,t}$		54.0
Compressive strength 1-direction	$S_{1,c}$		-521.8
Compressive strength 2-direction	$S_{2,c}$		-165.0
Shear strength	S_{12}		56.1

3.4 The cases considered

In addition to the experimental input needed to perform the PFA, the cases that have been considered should be outlined for a clear overview, in addition to other information that is relevant for the analysis and expectation of results, such as the fibre volume fraction. The cases will be presented in chapter-wise order, as has already been defined in Chapter 3.1.

Chapter 1: Unidirectional laminates under unidirectional loading

Table 3-2: Overview of unidirectional experiments performed as part of the Optimat project

Laminate	Lay-up	Abbreviation
UD tensile coupon	$[0_4]$	0-T
UD compressive coupon	$[0_4]$	0-C
UD off-axis tensile coupon	$[10_7]$	10-T
UD off-axis compressive coupon	$[10_7]$	10-C
UD off-axis tensile coupon	$[60_7]$	60-T
UD off-axis compressive coupon	$[60_7]$	60-C
UD transverse tensile coupon	$[90_7]$	90-T
UD transverse compressive coupon	$[90_7]$	90-C
Angle ply tensile coupon	$[45/-45]s$	45s-T

Chapter 2: Multidirectional laminates under unidirectional loading

Table 3-3: Overview of multidirectional experiments performed as part of the Optimat project

Laminate	Lay-up	Abbreviation
MD2 tensile coupon	[(45/-45/0)4 / 45/-45]	0-MDT
MD2 compressive coupon	[(45/-45/0)4 / 45/-45]	0-MDC
MD2 10-degree off-axis tensile coupon	[(55/-35/10)4 / 55/-35]	10-MDT
MD2 10-degree off-axis compressive coupon	[(55/-35/10)4 / 55/-35]	10-MDC
MD2 off-axis tensile coupon	[(105/15/60)4 / 105/15]	60-MDT
MD2 off-axis compressive coupon	[(105/15/60)4 / 105/15]	60-MDC
MD2 transverse tensile coupon	[(45/-45/90)4 / 45/-45]	90-MDT
MD2 transverse compressive coupon	[(45/-45/90)4 / 45/-45]	90-MDC

Chapter 3: Multidirectional laminate under biaxial loading

Table 3-4: Overview of bi-axial experiments performed as part of the Optimat project

Laminate	Lay-up	Abbreviation
MD2 1/0 cruciform	[(45/-45/0)4 / 45/-45]	1/0-T
MD2 0/1 cruciform	[(45/-45/0)4 / 45/-45]	0/1-T
MD2 0.5/1 cruciform	[(45/-45/0)4 / 45/-45]	0.5/1-T
MD2 0.925/1 cruciform	[(45/-45/0)4 / 45/-45]	0.925/1-T
MD2 1.925/1 cruciform	[(45/-45/0)4 / 45/-45]	1.925/1-T
MD2 2.7/1 cruciform	[(45/-45/0)4 / 45/-45]	2.7/1-T
MD2 5.4/1 cruciform	[(45/-45/0)4 / 45/-45]	5.4/1-T
MD2 7.7/1 cruciform	[(45/-45/0)4 / 45/-45]	7.7/1-T

3.5 Failure theories

The TS19101 describes two failure theories in Annex B.7.7 in detail, Tsai Hill and Tsai Wu criteria. Other well-established failure criteria, such as Hashin and Puck, are mentioned as alternatives to the criteria described. Generally, the criteria can be divided into several categories, interactive or non-interactive, depending on if the criterion considers the interaction between stresses in different directions, and mode-based or non-mode based, depending on if the criteria distinguish between mechanisms of failure. The pick of a suitable failure criterion needs careful consideration, as the choice will affect the outcome of the PFA. A simple criterion is easy to manage and fast in application, whereas a more advanced criterion could be able to describe the progression of failure more accurately. The dilemma was indicated by Hashin, who remarked that based on his experience, a linear criterion underestimates the strength of a material, whereas a higher degree polynomial is too complicated to manage [26].

In total, there are 26 experimental test cases to be considered from the OptiMat database [17], which will be split into UD coupons, multidirectional coupons, and cruciform coupons. The UD coupons will establish an understanding of the process, as well as basic rules of application, which will be followed throughout the thesis. The method will be further calibrated through application on multidirectional laminate loaded in compression and tension with different cut-off angles.

3.5.1 Tsai Wu

The Tsai-Wu (T-W) failure criterion is based on the general quadratic failure criterion adapted to polymer composites. It can be expressed in the form:

$$f = F_1\sigma_1 + F_2\sigma_2 + F_{11}\sigma_1^2 + F_{22}\sigma_2^2 + F_{66}\tau_{12}^2 + 2F_{12}\sigma_1\sigma_2 \qquad [3\text{-}1]$$

Where:

$$F_1 = \frac{1}{\sigma_{1,t}} - \frac{1}{\sigma_{1,c}};\ F_2 = \frac{1}{\sigma_{2,t}} - \frac{1}{\sigma_{2,c}};\ F_{11} = \frac{1}{\sigma_{1,c}\sigma_{1,t}};\ F_{22} = \frac{1}{\sigma_{2,c}\sigma_{2,t}}; \qquad [3\text{-}2]$$

$$F_{66} = \frac{1}{\tau_{12}^2};\ F_{12} = -\frac{1}{2}\sqrt{F_{11}F_{22}} \qquad [3\text{-}3]$$

The Tsai Wu criterion was one of the earliest failure criteria proposed for materials that exhibit anisotropic behavior such as composites. Despite being criticized as being non-

phenomenological, it has achieved success among engineers and researchers, being employed in design phases and incorporated in FE codes and textbooks. Optimizing the properties of the failure theories, such as the determination of the interactive strength parameter F_{12}, is not considered part of the scope of this research. Therefore, the interactive coefficient F_{12} has been set to $F_{12} = -\frac{1}{2}\sqrt{F_{11}F_{22}}$ [27].

Furthermore, Tsai Wu does not consider failure mode, which is necessary for analyzing damage progression. As it is not possible to know which mechanism of failure, any failure detected by Tsai Wu will be interpreted as fiber failure.

3.5.2 Hashin

Hashins criteria is a criterion able to distinguish between two failure modes in the composite laminate, one associated with the fibre and the other associated with the matrix. Hashins thoughts on the failure plane orientation being a function of applied stress state have inspired the making of more complex theories, however, it is to be noted that the author has used logical reasoning to produce the criterion, rather than to establish macro variables associated with the mechanisms of failure [26]. The criteria is formulated in terms of four stress invariants, which can be interpreted as four criteria for tensile fiber failure, compressive fiber failure, tensile matrix (transverse) failure, and compressive matrix (transverse) failure. The formulation looks like this:

Fiber tensile failure:

$$FF_t = \left(\frac{\sigma_1}{S_{1,t}}\right)^2 + \alpha\left(\frac{\tau_{12}}{S_{12}}\right)^2 \qquad [3\text{-}4]$$

Fiber compressive failure:

$$FF_c = \left(\frac{\sigma_1}{S_{1,c}}\right)^2 \qquad [3\text{-}5]$$

Matrix (transverse) tensile failure:

$$MF_t = \left(\frac{\sigma_2}{S_{2,t}}\right)^2 + \left(\frac{\tau_{12}}{S_{12}}\right)^2 \qquad [3\text{-}6]$$

Matrix (transverse) compressive failure:

$$MF_c = \left(\frac{\sigma_2}{2S_{12}}\right)^2 + \left[\left(\frac{S_{2t,c}}{2S_{12}}\right)^2 - 1\right]\left(\frac{\sigma_2}{S_{2,c}}\right)^2 + \left(\frac{\tau_{12}}{S_{12}}\right)^2 \quad [3\text{-}7]$$

Some limitations and incoherencies are recognized by the author, and even though it is a 3D criterion, the scope has been limited to UD laminates [28].

3.5.3 Tsai Hill

The Tsai Hill criterion is an extension of the Von Mises criterion used for steel. In the composite world, Tsai Hill is considered a less advanced criterion than the Tsai Wu criterion, as Tsai Wu is a generalized version of Tsai Hill. Comparing the equations, observe that in case the compressive and tensile strength is equal, $S_{1,t} = S_{1,c}\ and\ S_{2,t} = S_{2,c}$ there will be no difference in the results of these two failure criteria [29].

$$\left(\frac{\sigma_1}{S_{1,t\ or\ cc}}\right)^2 + \left(\frac{\sigma_2}{S_{2,t\ or\ 2,c}}\right)^2 + \left(\frac{\sigma_{12}}{S_{12}}\right)^2 - \left(\frac{\sigma_1\sigma_2}{S^2_{1,t\ or\ 1c}}\right)^2 = 1 \quad [3\text{-}8]$$

3.6 Degradation models

Furthermore, three different degradation models have been described, total degradation, limited discount, and residual property, one of which is to be applied to the failed plies considering what type of failure is occurring. The failure of plies will be limited to two types of failure modes, matrix failure, and fiber failure. The TS19101 does not specify when to apply which degradation model, except for in the case of limited discount, in which it is stated which strength and stiffness properties are to be reduced in case of matrix failure, and to apply total degradation in case of fiber failure. Considering the degradation models found in the literature, the following four models will be applied in case matrix failure is detected in a ply:

- Total Discount
- Limited Discount TS
- DNV Analytical
- Residual Discount.

Where Limited discount TS and DNV Analytical can both be viewed as a version of a limited discount degradation model, with the only difference being how to treat the strength properties of a failed ply. Both Total Discount and Limited Discount TS are taken from the TS19101, whereas DNV Analytical is from the DNV standard "DNV-ST-C501 Composite components". Lastly, the Residual Discount model is taken from literature in which it was successfully applied to predict progressive failure in a an FRP laminate with a circular hole [30]. Table 3-1 shows an overview of the reduction to be applied to the ply properties in case of matrix failure, note that in case of fiber failure, Total Discount is always applied.

Table 3-5: Reduction of material properties in case of matrix failure of ply

Matrix failure	Total Discount	Limited Discount TS	DNV Analytical	Residual Discount
E1	100%	-	-	-
E2	100%	100%	100%	55%
G12	100%	100%	100%	65%
V12	-	-	-	70%
Xt	100%	-	-	-
Xc	100%	-	-	-
Yt	100%	100%	-	-

Yc	100%	100%	-	-
S	100%	100%	-	-

3.7 Limitations in assessment of failure

The PFA will be applied with the Tsai Wu, Tsai Hill and Hashin, combined with the Total Discount, limited discount and residual discount degradation models. In total, this process will yield 12 predictions for each test case. Presenting each one of the predictions in a detailed manner including graphs would take up a large amount of space. Therefore, a table will be presented summarizing all the results, and a selected few of these will be presented with more details depending on the relevance.

[Blank page]

4 Unidirectional laminate under UD loading

This chapter aims to build a basic understanding of the PFA using the method as described in TS19101 as a framework, by predicting the failure of UD - and [45\-45]s-coupons. This will help in further developing the method to simulate the behavior of a multidirectional laminate under static tensile or compressive loading to obtain a more economical design. The predictions are produced and compared to UD beamlike coupon test results obtained from the OptiMat project. The UD experiments discussed in this Chapter were used to obtain the ply property data used as input in the predictions throughout the thesis mentioned in Table 3-1. The laminates are built by plies with a standard nominal ply thickness of 0.88 mm. From this, it follows that the nominal thickness of the whole laminates should be either 3.52 or 6.16, depending on if the laminate consists of four or seven layers.

This chapter will begin with introducing the experiments and results to be considered in each subchapter. The introduction will be followed by a presentation of the predictions through PFA, starting with Tsai Wu, and moving on to Tsai Hill and Hashin. Thereafter, a discussion will ensue regarding the results, to investigate the reason behind the inaccuracy. Finally, the chapter will end with exploring possible improvements to the PFA method within the framework of the TS19101. The chapter will start with on-axis coupons in Chapter 4.1, followed by off-axis coupons in Chapter 4.2, and lastly the [45/-45]s-laminate in Chapter 4.3.

4.1 On-axis coupons

A number of experiments were carried out on UD specimens in tension and compression as part of the OPTIMAT project. Table 4-1 includes an overview of the UD tests found in the OptiDat database, of which the first four in Table 4-1, (i.e. 0-T, 0-C, 90-T, 90-C, hereby: UD on-axis) coupons in the table are to be discussed in this subchapter. [19]

Table 4-1: Overview of unidirectional experiments carried out during the OPTIMAT project

UD on-axis test specimen					
Specimen	T or C	Cut-off Angle	Lay-up	Material	Abbreviation
UD	Tension	0	$[0]_4$	Combi 1250	0-T
UD	Compression	0	$[0]_4$	Combi 1250	0-C
UD	Tension	90	$[90]_7$	Combi 1250	90-T
UD	Compression	90	$[90]_7$	Combi 1250	90-C

UD off-axis test specimen (Hereby: UD-off-axis)					
UD	Tension	10	[10]7	Combi 1250	10-T
UD	Compression	10	[10]7	Combi 1250	10-C
UD	Tension	60	[60]7	Combi 1250	60-T
UD	Compression	60	[60]7	Combi 1250	60-C

Table 4-2 shows a summarization of the average test results for each experiment, including the measured thickness. [19]

Table 4-2: Summary of experiments on unidirectional coupons during the OPTIMAT project

Experiment*	Thickness [mm]	Fmax [kN]	Stress [MPa]	Strain [%]
0-T	3.752	72.49	776.50	2.091
0-C	3.817	-51.05	-525.91	-1.417
90-T	6.323	8.59	53.95	0.422
90-C	6.331	-26.24	-165.02	-1.9975
10-T	6.204	61.61	393.93	1.565
10-C	6.161	-58.75	-378.99	-1.466
60-T	6.137	11.2	72.23	0.802
60-C	6.110	-23.76	-154.41	-2.480

The experiments can be simulated by PFA, to determine when the failure of the laminate is predicted to happen. Thereafter, the predictions can be compared to the experimental results to determine the inaccuracy of the combination of a series of failure theories and degradation models. The predictions by use of Tsai Wu failure criterion combined with the Total Discount degradation model are summarized in Table 4-3 below.

Table 4-3: Comparison of experimental and Tsai Wu predictions on unidirectional coupons

UD coupons, Tsai Wu, Total Discount					
	Experimental results		Predicted results		Difference Stress|Strain
Coupon	Stress [MPa]	Strain [%]	Predicted Stress [MPa]	Predicted Strain [%]	Difference Stress|Strain

0-T	776.50	2.091	776.5	1.9895	0 % | 5 %
0-C	-525.91	-1.417	-521.9	-1.3367	1 % | 6 %
90-T	53.95	0.422	53.9	0.383	0 % | 10 %
90-C	-165.02	-1.9975	-165	-1.1728	0 % | 70 %

The predictions for UD coupons are very accurate in stress compared to the experimental results for all cases. There is a slightly larger inaccuracy for the strains, bar the 90-C, which exhibits significant deviation in the strain prediction when compared to the experiment. Tsai Wu is not able to distinguish between failure modes, therefore, Total Discount is the only model that has been applied in this case. The case of Tsai Hill and Hashin is similar to that of Tsai Wu, a single failure is achieved, resulting in a linear behavior. The results are summarized in Table 4-4:

Table 4-4: Summary of predictions on on-axis experiment

0-T				
Criterion	Total Discount	DNV Analytical	Residual Discount	Exp.
Tsai Wu	776.5	No pred.	No pred.	776.50
Tsai Hill	776.5	No pred.	No pred.	
Hashin	776.5	No pred.	No pred.	
0-C				
Tsai Wu	-521.9	No pred.	No pred.	525.9
Tsai Hill	-521.9	No pred.	No pred.	
Hashin	-521.9	No pred.	No pred.	
60-T				
Tsai Wu	53.9	No pred.	No pred.	53.95
Tsai Hill	53.9	No pred.	No pred.	
Hashin	53.9	No pred.	No pred.	
60-C				
Tsai Wu	-165	No pred.	No pred.	-165.02
Tsai Hill	-165	No pred.	No pred.	
Hashin	-165	No pred.	No pred.	

*No Pred. = No prediction

The first ply failure is interpreted to be the final failure of the laminate, therefore, only Total Discount is applied. No difference was found in the application of the different failure theories in the UD on-axis cases.

The predicted results fit very well with the experimental results, as was expected, because the stiffness and strength properties used as input in predicting the failure of the laminate, are the properties provided by the experiments. A difference is observed in the strains, particularly for the transverse compressive strain for the 90-C. The reason behind this inaccuracy becomes clear when investigating the stress-strain diagram provided by OPTIMAT. Figure 4-1 shows the experimental compressive test results on 0-C and 90-C laminates.

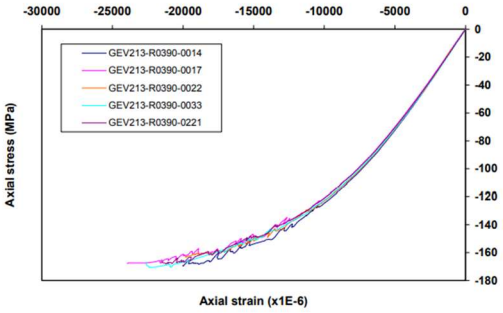

Figure 49. Axial stress vs. axial strain from coupons GEV213-R0390-0014, 0017, 0022, 0033, 0221 tested in compression

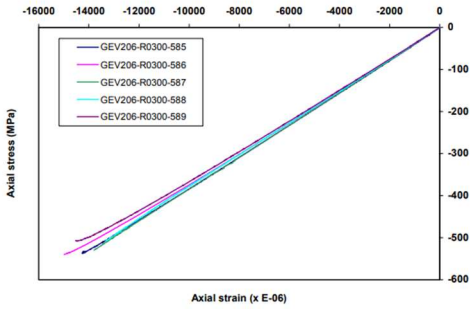

Figure 14. Axial stress vs. axial strain from coupons GEV206-R0300-0585 to 0589 tested in compression

Figure 4-1: Stress-strain plots of unidirectional coupons under compressive loading. On left: 90-C under compression. On the right: 0-C.

The nonlinearity is apparent in the experiment on 90-C under compression, but less so for the 0-C under compression. The prediction is not able to reproduce this non-linear behavior, as the first ply failure is deemed to be the final failure of the laminate. Reproducing the stress-strain graph of the 90-C under compression including the prediction in the visualization seen in Figure 4-2, the increased nonlinearity in 90-C compared to 0-C can be argued to be a result of loading in the matrix-dominated direction. The matrix is more ductile than the fibers and will show more nonlinear behavior as each crack reduces the stiffness under the transverse loading.

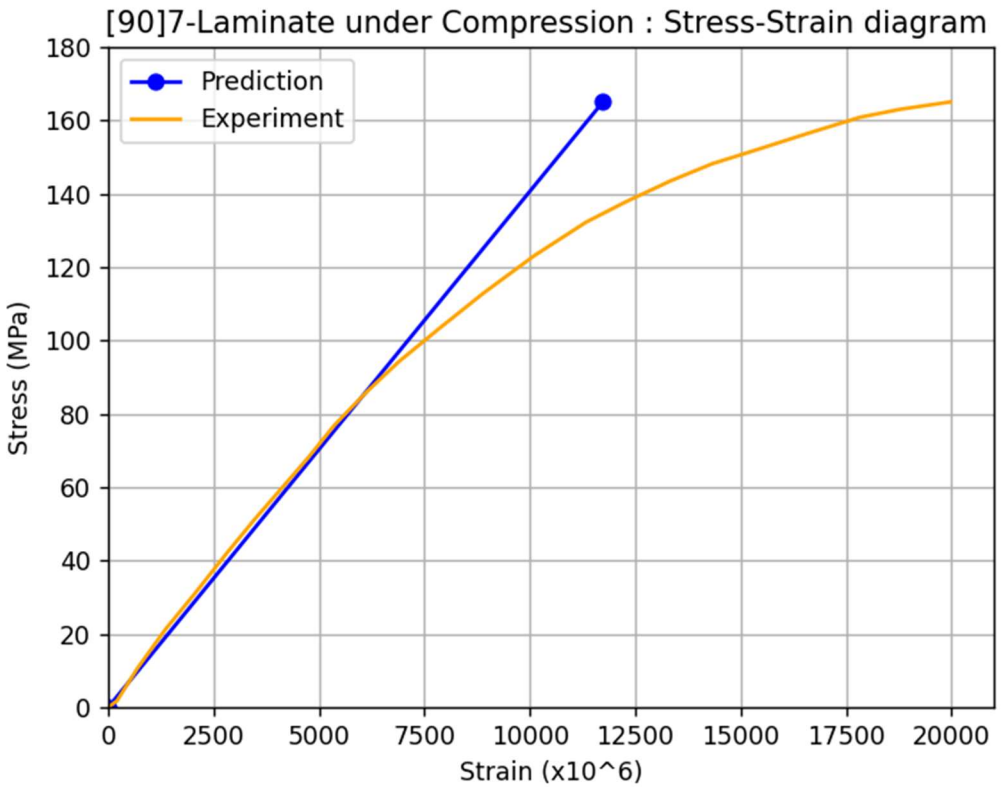

Figure 4-2: Stress-strain graph of 90-C laminate under compression. Experiment vs Prediction

Furthermore, it can be argued that the transverse specimen will not experience fiber rupture in a traditional sense, rather, out-of-plane failure or delamination is more likely to be the cause of failure. Thus, it is possible to consider the matrix failure to be the real failure of the laminate, as the prediction by Hashin criterion expects. Under an increasing load, the matrix will start cracking, reducing the support it is supposed to provide for the fibers. As the support continues to weaken, the fibers may be imagined being pulled out of position, resulting in delamination, and not rupturing, as it would if it was loaded in the fiber direction. For comparison, the experimental stress-strain graph of the transverse specimen in compression, are compared to the experiment in longitudinal compression, which displays linear behavior and more accurate strain prediction in Figure 4-1.

Some nonlinearity can also be observed in the 0-C, however, the stress will be better redistributed among the much stiffer fibers as the matrix cracks or a fiber snap. In the predictions, all plies (or fibers) facing the same direction will fail simultaneously, whereas this would likely not be the case in reality. A weakness in one fiber would likely lead to premature failure in one of the plies or fibers, and this would lead to a redistribution of stresses within the laminate. This will cause nonlinear behavior in laminates.

4.2 Off-axis coupons

Experiments on unidirectional off-axis (hereby: UD off-axis) coupons were performed as part of the OptiMat project. The tests were performed in both compression and tension, with two cut-off angles. A short overview of geometry and results can be seen in Tables 4-1 and 4-2. Table 4-5 provides an overview of the test results, compared to the Tsai Wu prediction.

Table 4-5: Comparison of UD off-axis experimental results and prediction with Tsai Wu and Total Discount

UD Off-Axis Coupon tests, Tsai Wu, Total Discount					
	Experimental results		PFA predictions		Difference Stress|Strain
10-T	393.93	1.565	308.60	0.9453	22 % | 40 %
10-C	-378.99	-1.466	-289.12	-0.8856	24 % | 40 %
60-T	72.23	0.8018	60.75	0.5046	16 % | 37 %
60-C	-154.41	-2.480	-137.50	-1.142	10 % | 54 %

A significant difference is observed between the predictions and the experimental results, as shown in Table 4-5, with Tsai Wu being conservative in all cases. In Figure 4-3, the comparison of experimental predicted results is visualized by plotting all four results.

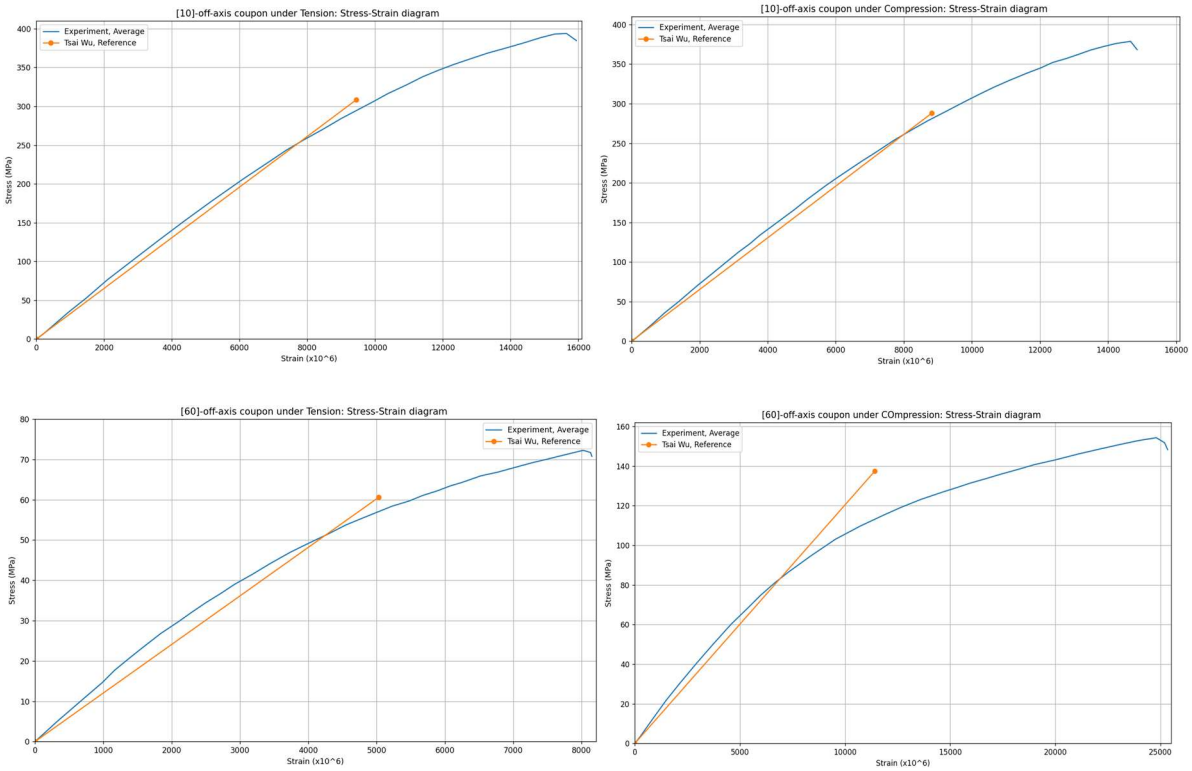

Figure 4-3: Stress-Strain plots of off-axis coupons, experimental (blue) and predicted (orange) results

The limitation of the predictions is visible as it is not able to incorporate the nonlinearity of the experimental results. The reason for no secondary failure is that the individual ply stresses are not redistributed after applying a degradation model to the failed plies, no change in the individual ply stresses means no change in the input to the failure theories. Therefore, no difference is observed with the different degradation models in the case with UD coupons, as is displayed in Table 4-6.

Table 4-6: Overview of predictions of off-axis coupons, all numbers in N/mm^2

10-T				
Criterion	Total Discount	DNV ANalytical	Residual Discount	Experiment
Tsai Wu	308.6	No pred.	No pred.	393.9
Tsai Hill	300.0	No pred.	No pred.	
Hashin	303.6	No pred.	No pred.	
10-C				
Tsai Wu	289.1	No pred.	No pred.	379.0
Tsai Hill	281.5	No pred.	No pred.	
Hashin	338.5	No pred.	No pred.	
60-T				
Tsai Wu	60.8	No pred.	No pred.	72.2
Tsai Hill	63.0	No pred.	No pred.	
Hashin	63.0	No pred.	No pred.	
60-C				
Tsai Wu	137.5	No pred.	No pred.	154.4
Tsai Hill	112.0	No pred.	No pred.	
Hashin	126.6	No pred.	No pred.	

Compared to the experiments, all predictions are conservative by 10 – 25 %. For the 10-T, no improvement is achieved by using a different failure theory, whereas under compression, only Hashin offers an improvement in prediction over the other failure criteria. As for the 60-T, a minor advantage is possible with Tsai Hill or Hashin, whereas under compression, no benefit is gained by swapping the failure theories.

Considering the results, the is no clear recommendation to be made. The accuracy of the considered failure theories is not sufficient to offer improvements in predictions by the PFA. A

possible solution could be the development of a specialized theory that can predict the off-axis cases based on on-axis experiments.

4.3 The angle ply

Experiments loaded in tension have been carried out on the [45/-45]s-laminate (Hereby 45s-T). Prediction by Tsai Wu and experimental result are presented in Table 4-7. The thickness used in the PFA is 0.955 mm per ply, with a total thickness of 3.82 mm for the laminate, corresponding to the average thickness of experiments.

Table 4-7: PFA predictions with Tsai Wu and Total Discount compared with the experimental result

	Stress [MPa]	Strain	Shear strain
Prediction	90.31	0.006763	0.010667
Experiment	112.14	0.018	0.03386
Difference	20 %	63 %	69%

A significant gap is observed between the predicted and the experimental results, 20 % difference in the stress prediction, and 60 % in the prediction of strain. The prediction is visualized in Figure 4-4. Considering the large inaccuracy, applying total degradation to the plies after initial failure seems rather punitive.

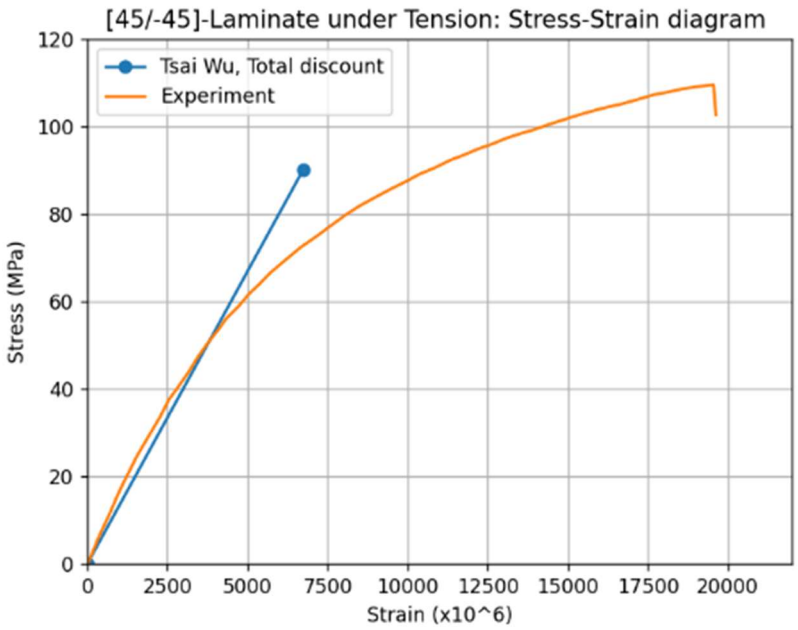

Figure 4-4 Stress strain graph of the experimental and the predicted result

Furthermore, studying the visualization, the failure might be interpreted as the initiation of matrix cracking of the laminate and not the final failure of the laminate. This interpretation is supported by Hashin, which interprets the initial failure of the laminate to be a matrix failure, and a much-improved prediction and visualization is achieved, see Figure 4-5 for a summary

of the predictions. Tsai Hill, like Tsai Wu, is not able to distinguish between matrix and fiber failure, as such, the resulting prediction is similar with both failure theories.

Table 4-8: Summary of the predictions for 45s-T laminate

45s -T					
Criterion	Total Discount	Limited Discount TS	DNV ANalytical	Residual Discount	Experiment
Tsai Wu	90.3	No pred.	No pred.	No pred.	112.1
Tsai Hill	95.3	No pred.	No pred.	No pred.	
Hashin	95.6	95.6	107.3	111.1	

Applying a failure theory able to predict matrix failure of a laminate, i.e. Hashin, decreases the inaccuracy of prediction from approximately 20%, down to 1%. The predictions achieved with Hashin in combination with residual discount are visualized in Figure 4-5.

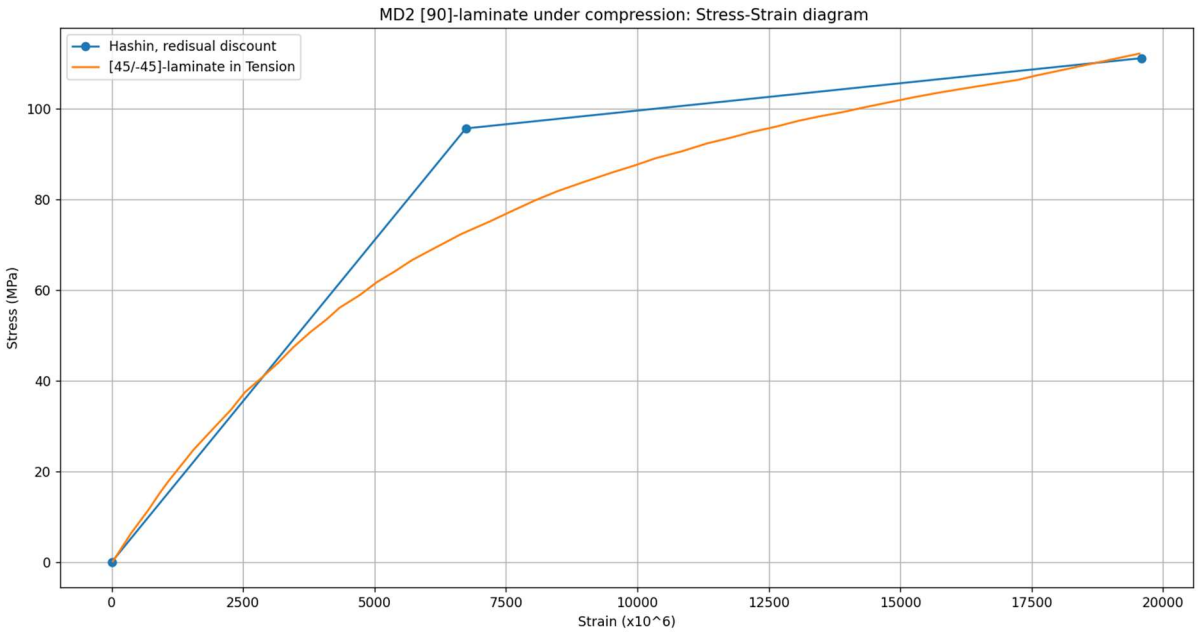

Figure 4-5: Plot of 45s-T specimen, experimental result, and prediction with Hahsin and Residual discount

Compared to Tsai Hill and Tsai Wu, Hashin offers a large improvement in the accuracy due to the ability to differentiate between failure modes.

4.4 Review of the method

Reviewing the method, there is a possibility of increasing the accuracy of Tsai Wu and Tsai Hill, if the criteria can distinguish between a failure in the matrix and in the fiber. Such interpretations do exist in literature. In DNVGL-ST-C501[8], chapter 6.4.2.3, the following recommendation is made in the guidance note, to predict matrix failure with Tsai Wu:

"... The Tsai-Wu criterion can be used instead to check for matrix cracking, if the following modifications are made to the strength parameters:

- *The ply strengths in fibre direction may be chosen to be much (1000 times) higher than the actual values*
- *The interaction parameter f12=0 shall be set to 0." (DNVGL-ST-C501, 2022)*

Exploring literature, a more general approach called "*failure indices*" is found. The idea behind failure indices is to separate between the individual stress contribution in the x-direction and y-direction. If the larger individual stress contribution to failure is in the y-direction, which is the matrix-dominated direction, this failure can be interpreted as a failure in the matrix. Whereas if the individual ply stresses show a larger contribution in the x-direction, the fibre-dominated direction, failure can be interpreted as fiber failure. To identify the failure mode with the Tsai Wu criterion, Equations 4-1 and 4-2, the individual contributions of the stress terms to the failure prediction can be separated into Equations 4-3 and 4-4, which contain all the terms in the main and the transverse directions, respectively. Comparing Equations 4-3 and 4-4, it is possible to interpret if the failure is in the matrix or in the fiber.

$$F_1\sigma_1 + F_2\sigma_2 + F_{11}\sigma_1^2 + F_{22}\sigma_2^2 + F_{66}\sigma_6^2 + F_{12}\sigma_1\sigma_2 = 1 \quad [4\text{-}1]$$

$$F_1 = \frac{1}{\sigma_1^T} + \frac{1}{\sigma_1^C}, F_2 = \frac{1}{\sigma_2^T} + \frac{1}{\sigma_2^C}, F_{11} = \frac{1}{\sigma_1^T\sigma_1^C}, F_{22} = \frac{1}{\sigma_2^T\sigma_2^C}, F_{66} = \frac{1}{\sigma_6^F\sigma_6^F} \quad [4\text{-}2]$$

$$H_1 = F_1\sigma_1 + F_{11}\sigma_1^2 \quad [4\text{-}3]$$

$$H_2 = F_2\sigma_2 + F_{22}\sigma_2^2 \quad [4\text{-}4]$$

A similar procedure can be followed for Tsai Hill, although simpler because of fewer terms in the criterion. Note that the shear term is left out, and a discussion regarding shear is not considered to be within the framework of this research. Applying this concept to 45s-T, the predictions can be updated as shown in Table 4-9:

Table 4-9: Update of prediction of 45s-T with failure indices applied to Tsai Wu and Tsai Hill criteria

[45/-45]s coupon under Tension					
Criterion	Total Discount	Limited Discount TS	DNV ANalytical	Residual Discount	Experiment
Tsai Wu	90.3	90.3	114.4	103.0	112.1
Tsai Hill	95.3	95.3	111.1	106.7	
Hashin	95.6	95.6	107.3	111.1	

Figure 4-6 shows the possible improvement by applying failure indices to Tsai Wu, with Tsai Hill showing a similar improvement in predicting capabilities. Failure indices will be further used in the next chapters in combination with Tsai Hill and Tsai Wu.

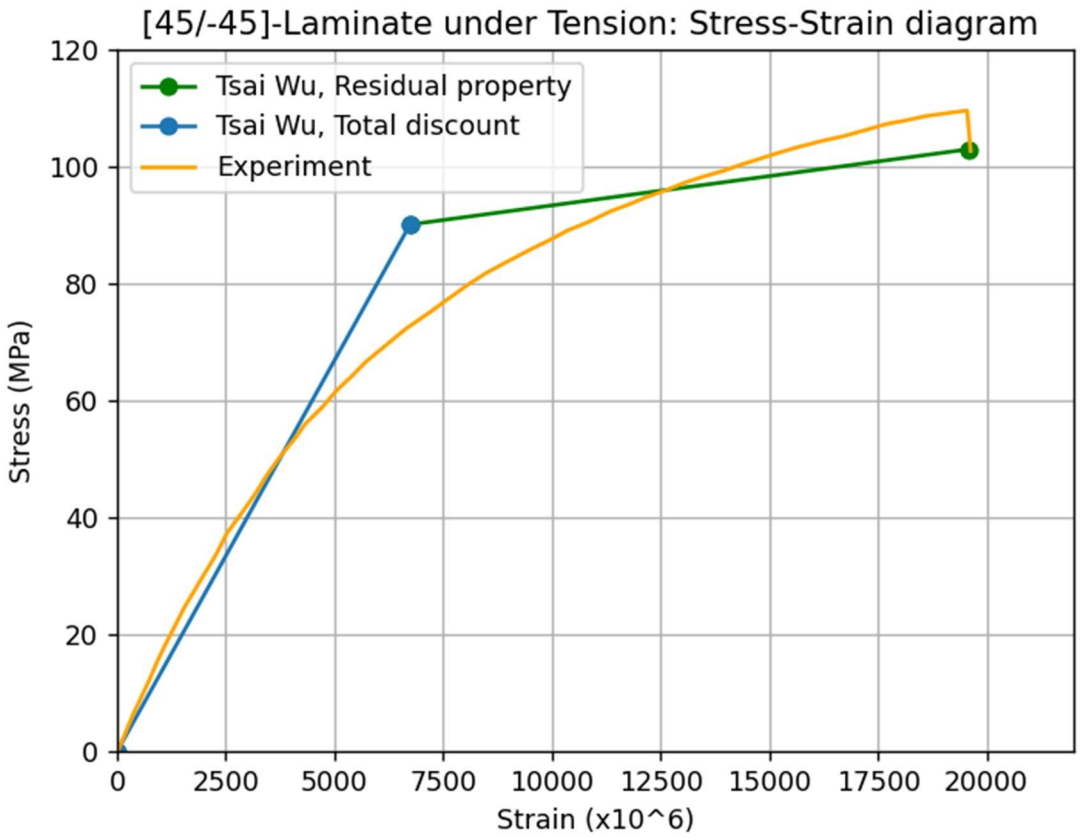

Figure 4-6: MD laminate under tension, prediction vs experiment

Furthermore, applying residual property reveals a particular problem for 45/s-T, as matrix failure is predicted to occur twice in a row. After FPF, the ply properties are reduced by the Residual Discount degradation model, leading to a redistribution of local ply stresses from the perpendicular to the parallel direction. However, the redistribution of transverse stresses is not large enough, and the failure theories interpret a second matrix failure to occur in the 45-plies, after the initial matrix failure of the 45-plies. All plies of the laminate fail simultaneously in matrix failure both times. Using Hashin as an example, in which the only difference between tensile matrix failure and tensile fiber failure are the terms $\frac{\sigma_{xx}}{Xt}$ and $\frac{\sigma_{yy}}{Yc}$, three possible solutions can be considered:

I) Consider matrix failure final failure:

After FPF, apply Residual Discount to matrix failure. If **all plies** of the laminate reach matrix failure a second time, consider the second matrix failure the final failure of the laminate.

II) Reapply Residual Discount:

After FPF, apply Residual Discount to matrix failure. When the laminate reaches secondary matrix failure, reapply Residual Discount by reducing the stiffness properties one more time. Keep repeating the reduction of stiffness until final failure is reached.

III) Manipulate the failure criterion:

After FPF, apply Residual Discount to matrix failure, and increase the transverse strength of the material, Y_c, by 1000. This will reduce the value of the $\frac{\sigma_{yy}}{Yc}$ term leading to matrix failure in Hashin, thereby eliminating the possibility of a secondary matrix failure. The next failure will then be fiber failure.

Considering the above options, I) considering matrix failure as the final failure, in case all the plies have failed, seems the most sensible option within the framework of this thesis, as it will be a conservative approach, and less time consuming than options II) and III). Going further in this thesis, matrix failure will be considered the dominant failure mode in the event all plies reach matrix failure a second time. Therefore, only one reduction will be applied due to matrix failure, and the analysis will be stopped when the last ply in the laminate reaches the matrix failure a second time.

4.5 Conclusion

No failure theory can perfectly describe the behavior of the laminate in failure in off-axis loaded specimens, however, it does show promise for a designer looking to approximate the behavior of a UD laminate. The designer should be aware that the input values are stress based, and even though the prediction regarding stress is accurate, the strain prediction does not show the same amount of accuracy. In case of a single failure, the prediction will show linear behavior, but this is only accurate for cases with loading in the high stiffness direction. In all other UD cases, the strain prediction will be conservative.

Both DNV Analytical and Residual Discount offer improved predictions with Hashin failure criterion for the 45s-T laminate, leading to the conclusion that the Total Discount is too severe in penalizing loss of stiffness and strength. However, the initial failure can be interpreted as coinciding with matrix failure when studying the visualization in Figure 4-6. Hashin criterion reinforces this assumption, allowing the possibility of improving the predictions by Tsai Hill and Tsai Wi with the application of failure indices to interpret the failure mode. With the less severe degradation models, a large increase in stress capacity is predicted.

Reviewing the degradation models, the two versions of limited discount – Limited Discount TS and DNV Analytical – do not add value to the discussion. The only difference between the two is the strength properties, and a discussion about the effect of this term is not deemed to be relevant to this thesis. Therefore, only DNV Analytical will be presented going forward.

5 Multidirectional laminate under UD loading

This chapter aims to build further on the understanding of the PFA gained in Chapter 4, by applying the procedure to a multidirectional laminate. This will help in understanding how the PFA procedure works in complex situations. The main purpose of this chapter is to determine the inaccuracy of the PFA for a multidirectional laminate under a loading applied in different directions by comparing the outcome with experiments from the OptiMat database. Thereafter, the reason behind the inaccuracy, solutions, and recommendations will be discussed. Lastly, a summary will be provided in the form of a conclusion.

5.1 Multidirectional laminate under tension

The multidirectional laminate consists of the following lay-up [(45/-45/0)4 / 45/-45] (hereby MD2), where the 45-plies are made of laminae with a nominal thickness of 0.61 mm and the 0-plies are made of laminae with a nominal thickness of 0.88 mm. The resulting nominal thickness of the laminate thus becomes 6.57 mm. Table 5-1 shows the average geometrical properties for experiments with tensile and compressive loading, respectively.

Table 5-1: Summary of mean geometrical properties of tensile and compressive MD coupons used in experiments

	Width [mm]	Thickness [mm]	Area [mm]
Tensile loaded coupons			
Average	25.32	6.72	170.29
COV (%)	0.175	1.187	1.249
Compressive loaded coupons			
Average	25.26	6.787	171.42
COV (%)	0.532	1.918	1.763

The average experimental results are given in Table 5-2:

Table 5-2: Summary of mean experimental results from tensile and compressive tests

	Fmax [kN]	Stress [N/mm^2]	Strain [%]
Tensile loaded coupons			
Average	88.27	519.81	2.238
COV	1.691	1.188	1.070
Compressive loaded coupons			
Average	76.05	443.71	1.739
COV	1.604	1.600	5.195

Table 5-3 displays predictions by Tsai Wu and Total Discount:

Table 5-3: Experimental results and PFA prediction, comparison of initial and final failure

	Prediction	Experiment	Difference [%]
Initial failure of 45 plies– Total Discount applied			
Stress [MPa]	182.59	---	
Strain	0.006686	---	
Final failure of 0 plies– Total Discount applied			
Stress [MPa]	411.46	519.81	20.8
Strain	0.019893	0.02238	11.1

Visualization of the results in Table 5-3 can be seen in Figure 5-1.

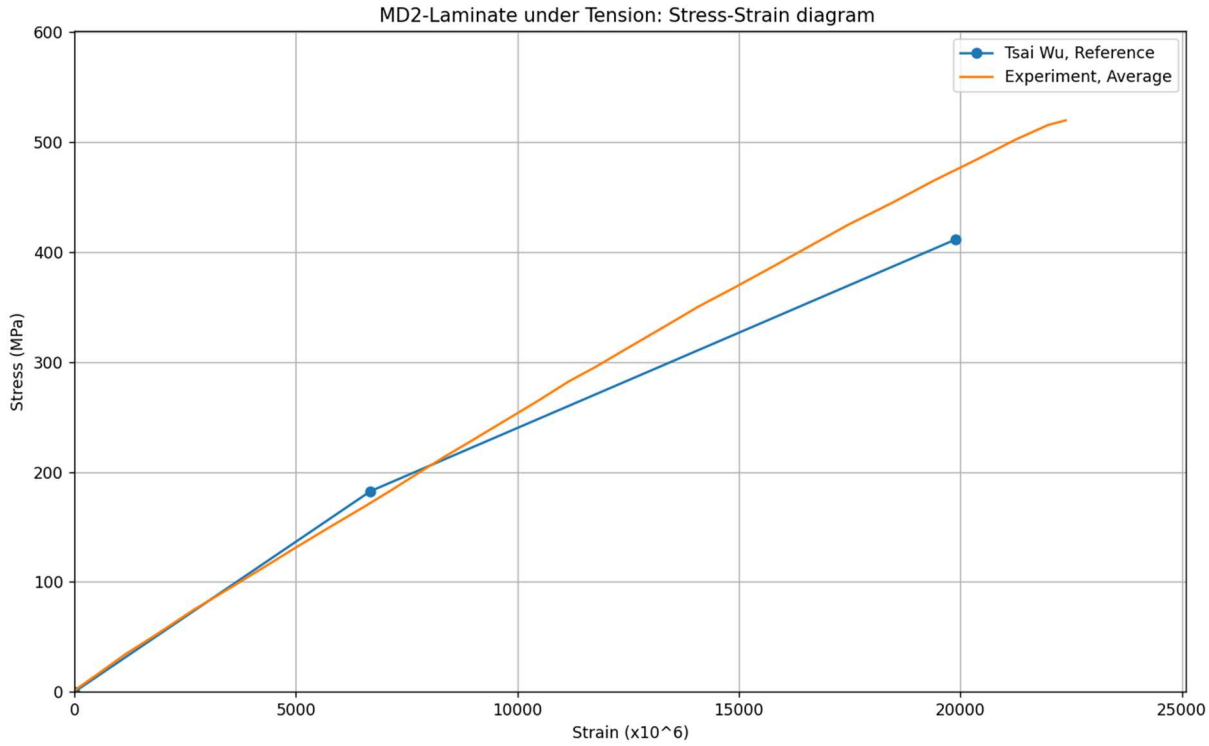

Figure 5-1: Visualization of PFA prediction and experimental results of MD2 laminate under tension on a stress-strain graph

The prediction has an inaccuracy of approximately 20 percent. Studying the visualization in Figure 5-1, the prediction can be observed to relate well with the experiment, however, the Total Discount model applies an overly severe reduction of stiffness. A less severe degradation model could increase the accuracy of predictions, and better simulate the behavior of the laminate. Applying the PFA on the laminate, including failure indices, a summary of the final failure predictions can be found in Table 5-4 and 5-5, in MPA and percentages, respectively.

Table 5-4: Summary of predictions on MD2 specimen compared to experimental result

0-MDT: MD2 coupon under tension [N/mm^2]				
Criterion	Total Discount	DNV ANalytical	Residual Discount	Experiment
Tsai Wu	411.5	378.0	427.7	519.8
Tsai Hill	411.5	393.6	439.9	
Hashin	411.3	453.0	487.7	

Table 5-5: Inaccuracy of each prediction compared to experimental result on MD2 specimen

0-MDT: MD2 coupon under tension [%]				
Criterion	TD	DNV analytical	RD	Exp.
Tsai Wu	20%	27%	17%	519.8
Tsai Hill	20%	24%	15%	
Hashin	20%	13%	6%	

The prediction of FPF, failure of the 45-plies, is similar for every failure theory. The failure of 45-plies can be interpreted as matrix failure in the case of Tsai Hill and Tsai Wu, which is supported by Hashin, also predicting matrix failure as FPF in the 45-plies. The secondary failure is fiber failure of 0-plies, after which not enough residual capacity is left for the laminate to carry a larger load. Unexpectedly, DNV Analytical shows a reduction of stress capacity compared to Total Discount, with only Residual Discount providing an improvement when applied to the failed plies. This pattern is only visible for Tsai Wu and Tsai Hill, whereas Hashin seems to increase the stress capacity as expected.

Hashin provides a 10 percent improvement in stress capacity with DNV Analytical compared to Total Discount. Moreover, considering Redisual Dicount model, a 20 percent improvement is achieved. A visualization of the results with Hashin can be summarized in Figure 5-2

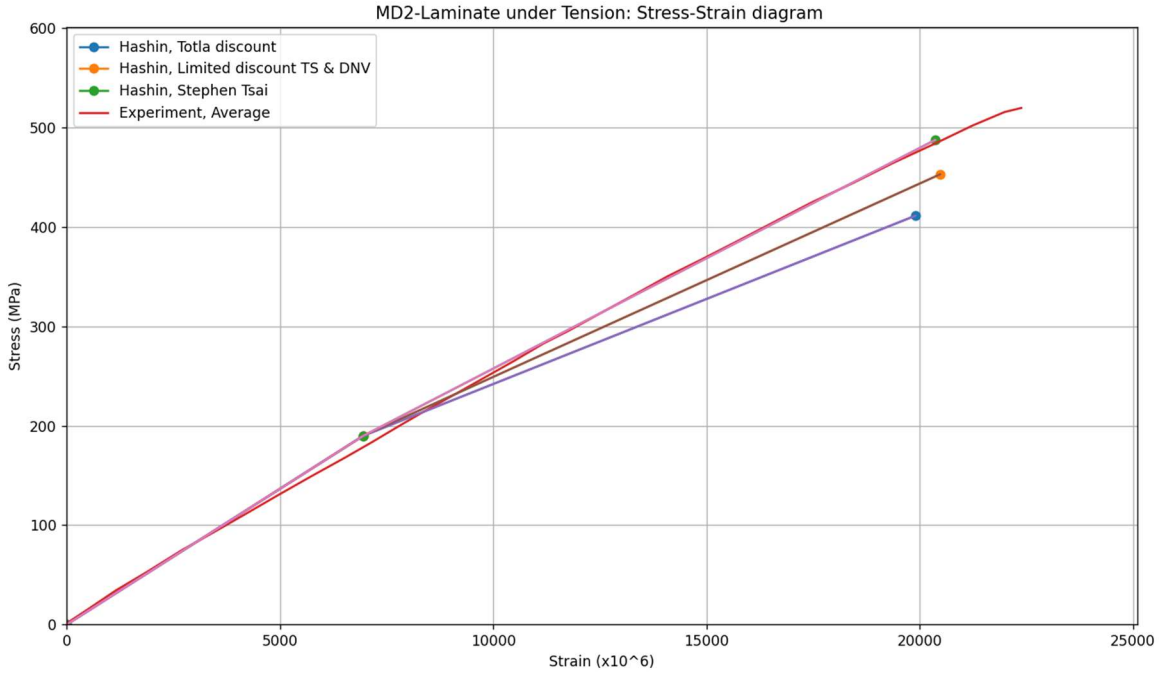

Figure 5-2: PFA of MD2 laminate under tension with Hashin criterion, combined with different degradation models

Hashin combined with Residual Discount provides a good representation of the laminate behavior and is 6 % conservative compared to the experiment. To summarize possible improvements of results when the failure theories are combined with Residual discount, a comparison is made to the combination of Tsai Wu and Total Discount, see Table 5-6. Hashin outperformes both Tsai Wu and Tsai Hill in terms of accuracy. Total Discount and DNV analytical models are left out as no improvement were offered.

Table 5-6: Improvement that can be achieved if failure theories are combined with the Residual Property model

	Tsai Wu, Total Discount	Tsai Wu, Residual property	Tsai Hill, Residual property	Hashin, Residual property
Improvement from Tsai Wu, Total Discount by:	0 %	4 %	7 %	19 %
Conservative to experiment by:	20 %	17 %	15 %	6 %

Considering the failure theories, Tsai Hill and Tsai Wu both end up with non-expected results for the Limited Discount degradation model. Total Discount was anticipated to give the lowest results in terms of stress capacity due to its severe nature, however, with DNV analytical, a reduction of stress capacity is observed from Total Discount.

The cause of this is unclear, but an explanation can be given by looking at the individual ply stresses considering how the stresses are redistributed for the two degradation models after a ply fails. When Total Discount is applied, the individual ply stresses in the 45-plies are reduced to zero, in the x-direction and the y-direction direction. Therefore, the 45-plies have no contribution to the PFA after failure when Total Discount is applied. The remaining 0 plies, then act as a UD laminate and ply stresses only in the parallel direction remain, and only ply stresses in the x-direction are observed.

However, when DNV Analytical is applied, the individual ply stresses in the in the x-direction of the 45-plies remain, and only the perpendicular ply stresses of the 45-plies are reduced to zero. Because of the contribution of the 45-plies, individual ply stresses in both x- and y-direction can be observed in the 0-plies. Keeping this in mind, it is important to realize that the y-direction individual ply stresses will have a larger contribution to failure relative to the x-direction individual ply stresses, because the transverse tensile strength is only 54 N/mm^2, whereas the parallel tensile strength is 776 N/mm^2. Consequently, a reduction of stress capacity is observed when Limited Discount is applied with the interactive failure criteria, Tsai Wu and Tsai Hill. This effect is not seen in non-interactive criteria, such as Hashin, because the fiber failure equation is not dependent on ply stresses in the y-direction, rather, only ply stresses in the x-direction and shear stresses are considered for the prediction of fiber failure.

Considering the degradation models, Total Discount provides a 20% conservative result combined with any failure theory, whereas DNV Analytical provides an even lower stress capacity at final failure on average. It could be concluded that the limited discount degradation model provides the least satisfying representation of the matrix damage on the ply properties when combined with an interactive failure criterion.

Residual discount provides an increase of stress capacity in combination with all failure theories as is seen in Table 5-7, and is the most realistic and accurate model of degradation for the 0-MDT laminate. Note that only Hashin combined with RD shows a prediction less than 10% of inaccuracy.

The predictions give the impression that the laminate is overperforming in experiments, compared to what theory can predict through PFA. This could be an inherent conservatism in the failure theories, or the degradation models are too severe. Nevertheless, the results indicate that there is a strengthening physical interaction between the plies, increasing the stress capacity of the laminate which PFA is not able to capture.

A possible solution could be to consider a failure theory including a positive consequence of stress interaction between the plies in parallel and perpendicular direction. Tsai Hill and Tsai Wu which penalizes the interaction between x- and y-direction, whereas Hashin ignores it. However, note Hashin does considers an interaction between stresses in the x-direction and shear stress for tensile loaded cases.

To conclude, the discussion about which failure theory is the most realistic simulation of the experiments is not easy to settle, as a 2D model will always be limited. Interaction between the plies is expected, yet the failure criterion with the least amount of interaction, i.e. Hashin, provides the most satisfying results.

For MD2 laminate under tension, Tsai Hill will provide a 7% more accurate result than Tsai Wu, however, in both cases, Residual Discount and failure indices need to be applied. As an alternative, Hashin seems like the better choice. Hashin can predict the matrix failure of 45-plies without extra work related to interpreting matrix failure from individual ply stresses and offers an increase of 19% compared to Tsai Wu. In general, Hashin criterion is recommended for use in the case of 0-MDT laminate, combined with Residual Discount, as it is requires no additional work to be applied, all the while being only 6% conservative.

5.2 Multidirectional laminate under compression

The multidirectional laminate under compression is similar to the one under tension, the layup is [(45/-45/0)4 / 45/-45], where the 45-plies are made of plies with a nominal thickness of 0.61 mm, and the 0-plies are made of plies with a nominal thickness of 0.88 mm. The resulting nominal thickness of the laminate thus becomes 6.57 mm, whereas the actual average thickness of the laminate is 6.78 mm. Table 5-1 and 5-2 shows the average geometrical properties the compressive experiments. Table 5-7 displays a comparison between the failure prediction with Total Discount and the Total Degradation model, and the experimental result.

Table 5-7: Prediction of failure with Tsai Wu and Total Discount compared to experiment

	Prediction	Experiment	Difference [%]
Initial failure – Total Discount applied to 0 -lies			
Stress [MPa]	257.82	---	---
Strain	0.40913	---	---
Final failure – Total Discount applied to 45-plies			
Stress [MPa]	60.47	443.71	42%
Strain	0.9596	1.739	135%

The comparison shows a significant inaccuracy in predicted final failure, which is 42 % conservative compared to the experimental results. See visualization in Figure 5-3.

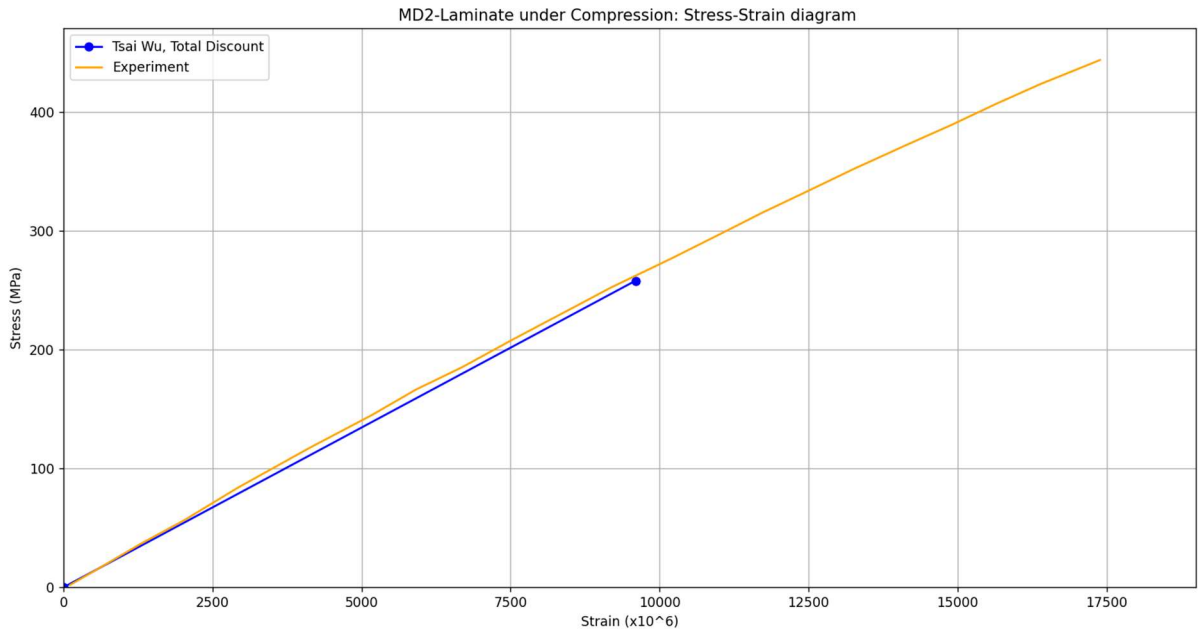

Figure 5-3: 10-MD2 laminate under compression, prediction vs experiment

Furthermore, FPF is predicted to be in the 0-plies, which contributes to the large inaccuracy. Table 5-8 and Table 5-9, display the results of the PFA, first in terms of stress and then in percentages, for every failure theory considered.

Table 5-8: Summary of predictions on MD2 specimen under compression compared to experiment

0-MDC: MD2 coupon under compression [N/mm^2]				
Criterion	TD	DNV analytical	RD	Exp.
Tsai Wu	257.8	257.8	257.8	443.71
Tsai Hill	277.4	236.9	251.0	
Hashin	277.43	305.6	329.2	

Table 5-9: Summary of prediction on MD2 under compression compared to experiment in percentage

0-MDC: MD2 coupon under compression [%]				
Criterion	TD	DNV analytical	RD	Exp.
Tsai Wu	42%	42%	42%	443.71
Tsai Hill	37%	52%	43%	
Hashin	37%	31%	25%	

Tsai Wu criterion interprets the initial failure of 0-plies as fiber failure. Thus, total degradation will be applied to the 0-plies, and the 45-plies do not have enough strength to carry more stress. Tsai Hill predicts failure of the 45-plies in the matrix as first ply failure, and a similar pattern as was observed in 0-MDT is observed. DNV Analytical offers a reduced capacity, however, even with Residual Discount, a reduced capacity of stress capacity is observed compared to Total Discount.

Hashin follows the same pattern as previously observed with 0-MDT. Significant improvement in prediction is possible, see Figure 5-4. However, the most positive result is still 25 % conservative in comparison to the experimental result.

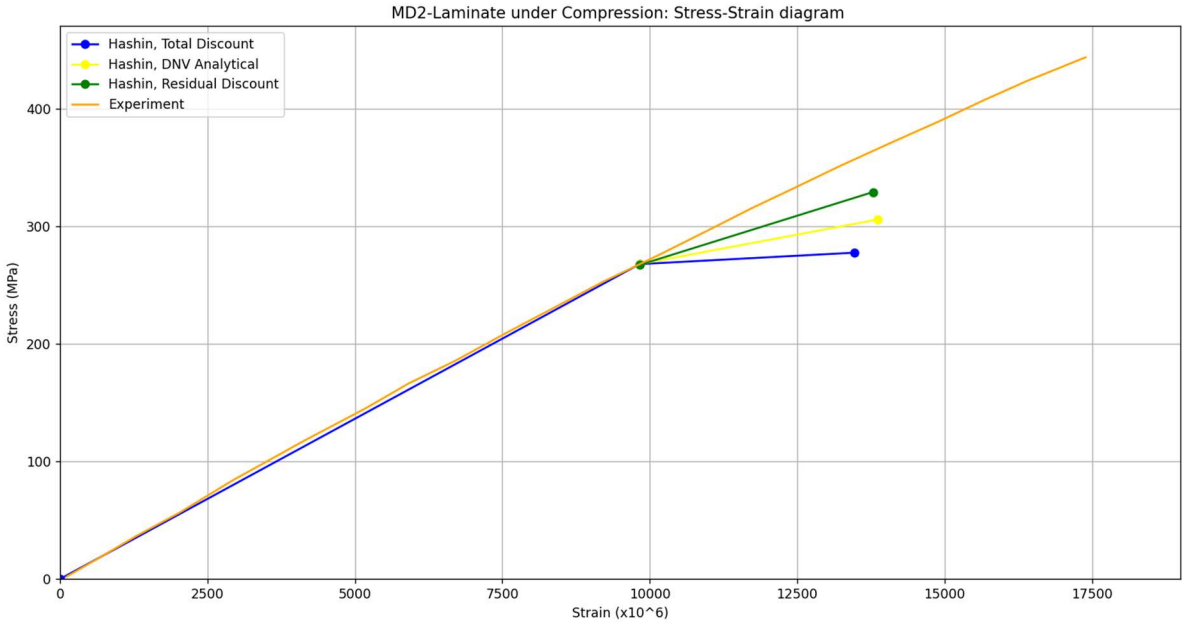

Figure 5-4 0-MDC, experiment vs prediction

Hashin improves the prediction significantly compared to the initial prediction in terms of stress capacity. **This leads to two conclusions**, firstly, the **failure criteria are less accurate for loading under compression** than under tension. Secondly, a **failure criterion that considers a stress interaction strengthening the laminate** might increase the stress capacity, thus raising the accuracy of predictions.

5.3 MD2 under transverse loading

Until now, the thesis has focused on results obtained in test phase two of the OptiMat project. However, as part of test phase 5 of the OptiMat project, the MD2 laminate was characterized through experiments in the transverse direction. The nominal thickness of the laminate is still 6.57 mm and the results for the laminate under tension and compression in the x-direction are similar to what has already been observed in test phase 2. Table 5-10 summarizes the test results:

Table 5-10: Summary of MD2 on-axis experimental results

0-MDT				
	σ_{xt}	E_{xt}	ϵ_{xt}	ν_{xt}
Average	518.9	16.4	2.29	0.485
St. Dev.	11.5	0.5	0.08	0.019
0-MDC				
	σ_{xc}	E_{xc}	ϵ_{xc}	ν_{xc}
Average	-469.5	25.2	-2.03	0.466
St. Dev.	9.0	2.2	0.07	0.037
90-MDT				
	σ_{yt}	E_{yt}	ϵ_{yt}	ν_{yt}
Average	143.9	15.1	2.90	0.275
St. Dev.	2.9	0.8	0.17	0.062
90-MDC				
	σ_{yc}	E_{yc}	ϵ_{yc}	ν_{yc}
Average	-199.6	14.4	-	0.256
St. Dev.	8.9	0.4	-	0.002
MD2 laminate under shear				
	τ_{xy}	G_{xy}	γ_{xy}	-
Average	147	8.1	2.65	-
St. Dev.	6	0.8	0.14	-

Predictions for the experiments loaded in the transverse direction can be summarized in Table 5-11 and Table 5-12.

Table 5-11: MD transverse specimen predictions, compared to experiments

MD2 coupon under transverse tension [N/mm^2]				
Criterion	TD	DNV analytical	RD	Exp.
Tsai Wu	59.4	162.9	156.8	143.9
Tsai Hill	60.7	165.4	138.4	
Hashin	60.9	162.9	146.4	
MD2 coupon under transverse compression [N/mm^2]				
Criterion	TD	DNV analytical	RD	Exp.
Tsai Wu	-179.4	-164	-204.57	-199.6
Tsai Hill	-143	-132	-184.6	
Hashin	167.6	-167.6	-226.18	

Table 5-12: MD transverse specimen predictions in percent difference, compared to experiments, negative are optimistic

MD2 coupon under transverse tension [N/mm^2]				
Criterion	TD	DNV analytical	RD	Exp.
Tsai Wu	59%	-13%*	-9%*	-143.9
Tsai Hill	58%	-15%*	4%	
Hashin	58%	-13%*	-2%*	
MD2 coupon under transverse compression [N/mm^2]				
Criterion	TD	DNV analytical	RD	Exp.
Tsai Wu	10%	18%	-3%*	199.6
Tsai Hill	28%	34%	8%	
Hashin	16%	16%	-13%*	

*Optimistic prediction

For transverse tension, the predictions have a significant conservatism, almost 60%, when combined with total discount, whereas the results are highly accurate, with less than 10% inaccuracy, for residual discount for all cases. However, note that both Tsai Wu and Hashin are

optimistic compared to the experiment, although within 5 % of deviation. Surprisingly, DNV Analytical predicts a larger stress capacity than Residual discount. FPF is considered to be in the 0-plies.

For transverse compression, Total Discount and DNV Analytical are conservative in combination with all failure theories. Residual Discount offers an increased stress capacity in all cases but is optimistic for both tension and compression when combined with Tsai Wu and Hashin. Tsai Hill remains conservative and highly accurate in both cases when combined with Residual Discount. The Hashin criterion is conservative for Total Discount but becomes optimistic for Residual Discount in both cases. FPF is considered to be in the 0-plies.

The predictions with residual discount are observed to be more optimistic than had been previously observed in 0-MDT and 0-MDC. As for the cause, it can be argued that as the MD2 laminate is pulled in transverse tension, the 0-plies will experience compressive strain perpendicular to the load direction, i.e. in the fiber direction. The compressive stress can be imagined having an unfavorable effect, as the compressive stress in x-direction will contribute to the buckling of fibers. This could lead to premature failure of the 0-plies, leaving the 45-plies to carry the load, thereby reducing the overall capacity of the laminate. Comparatively, the compressive stress in 0-MDC, may be imagined to be pushing the fibers together and providing additional support. Thereby, increasing the real capacity of the laminate, and increasing the inaccuracy achieved by the failure critria.

A general conclusion would be to exercise carefulness when failure theories and Residual Discount degradation model is applied to predict the behavior of a laminate in the matrix-dominated direction. Despite the inaccuracy being less than 10% in most cases, there is a risk of overpredicting the stress capacity of the laminate. Concluding the transverse cases, Tsai Hill can be recommended to be the most suitable failure theory for transversely loaded MD2 specimen.

5.4 MD2 – Off-axis specimen

This section deals with the same multidirectional laminate, MD2, [(45/-45/0)4 / 45/-45], as has been discussed in the previous subchapters, but with a cut-off angle of 10 and 60 degrees. Table 5-13 shows the geometrical properties:

Table 5-13: Overview of geometrical properties of MD2 off-axis beamlike coupons

	Width [mm]	Thickness [mm]	Area [mm]
10-MDT– 5 observations			
Average	25.137	6.445	162.27
COV (%)	0.410	0.342	0.629
10-MDC: – 5 observations			
Average	25.227	6.444	162.581
COV (%)	0.142	0.384	0.419
60-MDT: – 5 observations			
Average	25.246	6.488	163.797
COV (%)	0.220	0.788	0.945
60-MDC: – 5 observations			
Average	25.235	6.498	163.995
COV (%)	0.161	0.827	0.716

Table 5-14 displays an overview of the experimental results:

Table 5-14: Overview of experimental results of MD2 off-axis beamlike coupons

	Fmax	Stress	Strain
10-MDT– 5 observations			
Average	78.99	486.75	2.153
COV (%)	3.733	3.345	5.108
10-MDC: – 5 observations			
Average	70.36	432.76	1.722
COV (%)	2.889	2.788	5.211
60-MDT: – 5 observations			
Average	32.12	196.17	2.082
COV (%)	3.882	3.598	5.288

60-MDC: – 5 observations			
Average	41.12	250.77	1.890
COV (%)	1.932	2.412	2.031

Presenting detailed results for each one of these results with the PFA process applied will be an unnecessarily long procedure. Therefore, Table 5-15 provides a summary of the predictions.

Table 5-15: Summary of MD off-axis predictions compared to the experiment

10-MDT				
Criterion	TD	DNV analytical	RD	Exp.
Tsai Wu	227.1	357.1	394.3	486.75
Tsai Hill	227.1	339.6	373.4	
Hashin	235.4	361.5	389.2	
10-MDC				
Tsai Wu	265.8	265.8	265.8	432.76
Tsai Hill	226.2	232.6	263.8	
Hashin	258.9	325.2	349.7	
60-MDT				
Tsai Wu	78.0	163.8	217.25	196.17
Tsai Hill	80.1	167.08	211.52	
Hashin	80.1	167.08	214.31	
60-MDC				
Tsai Wu	206.3	206.3	206.3	250.77
Tsai Hill	184.0	184.0	184.0	
Hashin	200.6	200.6	200.6	

The predictions can be summarized in percentages in Table 5-16.

Table 5-16: Summary of MD off-axis predictions compared to experimental results, in percentages

10-MDT				
Criterion	TD	DNV analytical	RD	Exp.
Tsai Wu	53%	27%	19%	486.75
Tsai Hill	53%	30%	23%	
Hashin	52%	26%	20%	
10-MDC				
Tsai Wu	39%	39%	39%	432.76
Tsai Hill	43%	43%	39%	
Hashin	36%	25%	19%	
60-MDT				
Tsai Wu	60%	16%	-11%	196.17
Tsai Hill	60%	14%	-8%	
Hashin	59%	14%	-9%	
60-MDC				
Tsai Wu	18%	18%	18%	250.77
Tsai Hill	27%	27%	27%	
Hashin	20%	20%	20%	

Hashin criterion consistently predicts approximately 20% conservative results when combined with Residual Discount, except in the case of 60-MDT, in which the prediction is 20% optimistic. Tsai Wu and Tsai Hill are both less consistent than Hashin, however, all three theories struggle with optimism on the 60-MDT specimen.

To conclude, an MD2 laminate subject to a load at an angle of 10 degrees, will obtain a significant increase in accuracy for tensile loading by use of Residual Discount model instead of Total Degradation. Subject to compressive loading, only Hashin is able to improve the prediction.

The same conclusion can be made for the laminates subject to loading at an angle of 60 degrees, however, the tensile loaded case will end up overpredicting the stress capacity in every cases when combined with Residual Discount.

There is no convincing recommendation to be made based on these results, except that the engineer needs to be careful when considering cases involving an off-axis load. Even more so when this load is directed more towards the weak matrix dominated direction, as is the case with 60-MDT. Similar to the 90-MDT, there is a risk of overpredicting the laminates strength.

5.5 Review of the method

Because of the large number of test results considered in Chapter 5, a more complete overview can be produced using statistics and failure envelope. This will help in characterizing the results from a different point of view. Furthermore, the thesis aims to explore the PFA for design purposes, for which the 95 percentile lower confidence is required, not the mean values which are relevant when considering model validation [31]. To ensure that the predictions are always within the experimental test results, a model factor can be produced based on statistics. The model factor should be such that the designer can ensure the prediction is safe with 95 % certainty. Table 5-17 provides a summary of important statistical parameters.

Table 5-17: Statistical characterization of experimental results on MD2 laminate

	MD2 laminate under tension, Confidence level of 95 %			
	0-MDT	10-MDT	60-MDT	90-MDT
Mean	519.81	486,75	196,17	143,89
Std. Dev.	2,76	16,28	7,06	2,96
Upper 95%	527,5	506,97	204,93	146,63
Lower 95 %	512,1	466,53	187,41	141,16
	MD2 laminate under compression, Confidence level of 95 %			
	0-MDC	10-MDC	60-MDC	90-MDC
Mean	443,54	432,76	250,77	199,62
Std. Dev.	7,11	12,07	6,05	8,88
Upper 95%	451,00	447,75	258,28	210,65
Lower 95 %	436,08	417,78	243,26	188,60

The experimental results of MD2-laminate are plotted in Figure 5-5. The figure visualizes the mean results as circular dots and upper/lower bounds of the confidence interval with arrows. The x-axis represents individual ply stresses in the x-direction whereas the y-axis represents stresses in the y-direction.

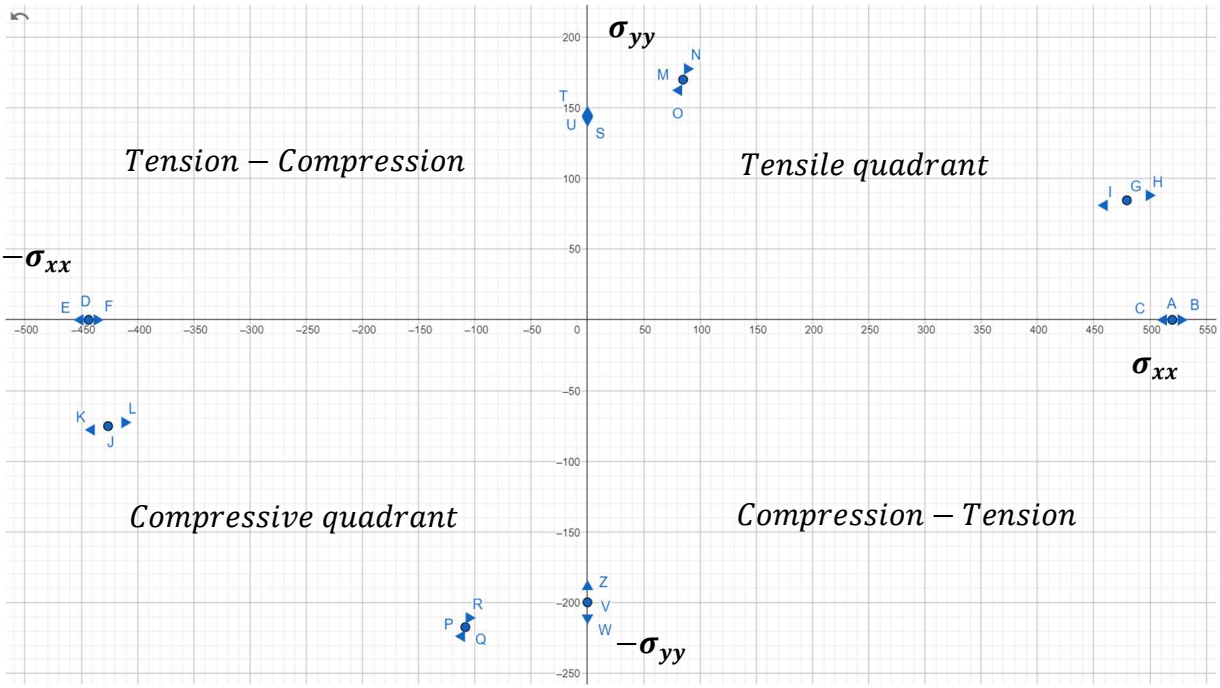

Figure 5-5: Failure envelope for MD laminate, visualized in the 4 quadrants. The mean value is represented by blue dots, and 95 percentile values are represented by arrows.

Studying Figure 5-5, an envelope can be imagined between the mean experimental values. Figure 5-6 visualizes the failure envelope for mean experimental results, in addition to the predictions. Total Degradation is represented by green dots, Residual Discount by red dots, and turquoise dots for overlap between the two. For the tensile and compressive predictions, part of the envelope can be observed to exceed the experimental envelope.

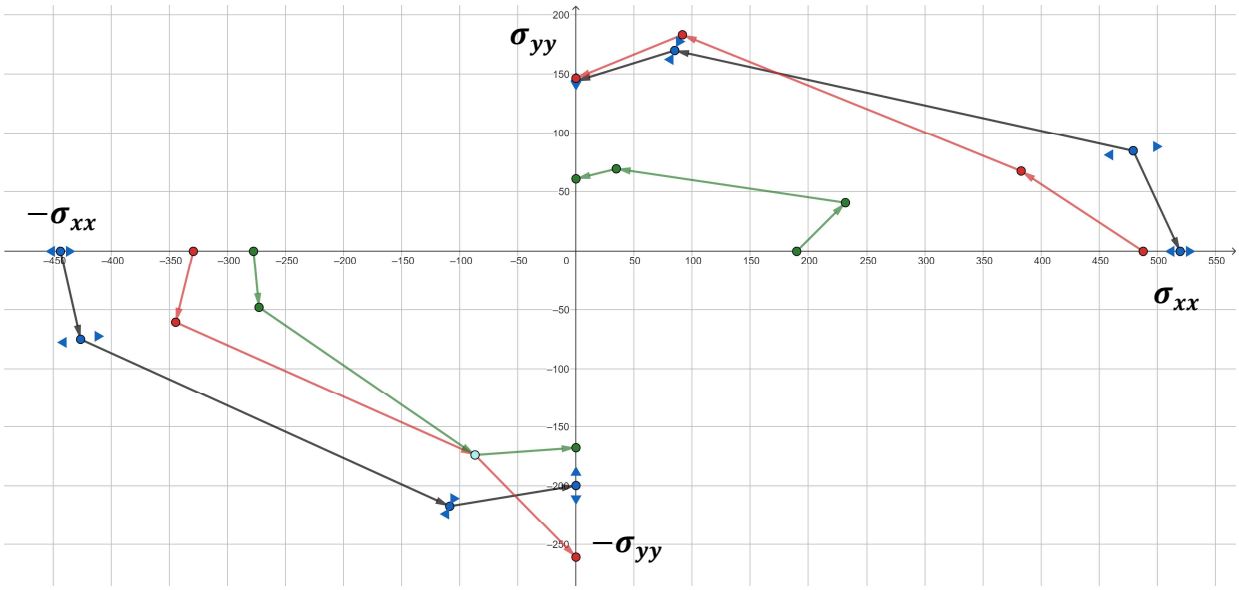

Figure 5-6: Failure envelopes for Hashin criterion, with color. Green: Total Discount. Red: Residual discount. Blue/black: Mean experimental result

Hashin is noted to predict a higher strength in transverse compression than it does for transverse tension by approximately 100 MPA. This can be attributed to the fact that Hashin includes the shear term for tensile fiber failure, see Equation 3-4, whereas compressive fiber failure only considers the compressive stresses, see Equation 3-5. Furthermore, Figure 5-6 visualizes the loss of conservatism as the load direction gravitates towards the y-direction. More off-axis experiments would have helped greatly in determining where this change takes place.

Table 5-18 provides an overview of the model factors that can be applied to ensure that the prediction is conservative with 95 % certainty.

Table 5-18: Proposed model factors to be applied to predictions with Residual Discount

	MD2 laminate under tension, Confidence level of 95 %			
	0-MDT	10-MDT	60-MDT	90-MDT
Tsai Wu	1.0	1.0	0.86	0.9
Tsai Hill	1.0	1.0	0.88	0.96
Hashin	1.0	1.0	0.87	0.96
	MD2 laminate under compression, Confidence level of 95 %			
	0-MDC	10-MDC	60-MDC	90-MDC
Tsai Wu	1.0	1.0	1.0	0.7
Tsai Hill	1.0	1.0	1.0	1.0
Hashin	1.0	1.0	1.0	0.72

Considering the model factors above, a reduction is necessary in the cases of the 60- and 90-MDT for every failure criterion to ensure conservative results with 95 % certainty. Whereas in compression, only Tsai Wu and Hashin would require a model factor in case of 90-MDC. Considering all failure theories combined with the residual discount model, a model factor of 0.7 should be used, which would lead to a rather large reduction of capacity. However, it is possible to divide the predictions into tension and compression, which means the largest tensile model factor is 0.86, whereas 0.7 is to be used for compression.

It would be possible to apply an ultimate strain criterion to reduce the optimistic predictions achieved through PFA. In reality, when a ply is reduced by residual discount, the residual stiffness should not offer the stiffness for an infinite amount of time. Rather, a continuous reduction is more sensible, given the gradual process of plies degrading as the load

increases. However, it would be time-consuming to apply a more gradual reduction than has already been applied. Therefore, it makes sense to apply a strain limit that the laminate should not be able to exceed. To make a judgment about the strain limit, the stress-strain graphs should be known, thereafter, it would be possible to apply a strain limit. The issue with the ultimate strain approach is that an accurate application requires knowledge prior to the analysis, which will not necessarily be available. Studying Figure 5-7 and making a comparison to the strain limit of a UD laminate under tension and compression in Table 4-2, a strain limit of 1.5% for compression, and 2 % for tension seem to be reasonable.

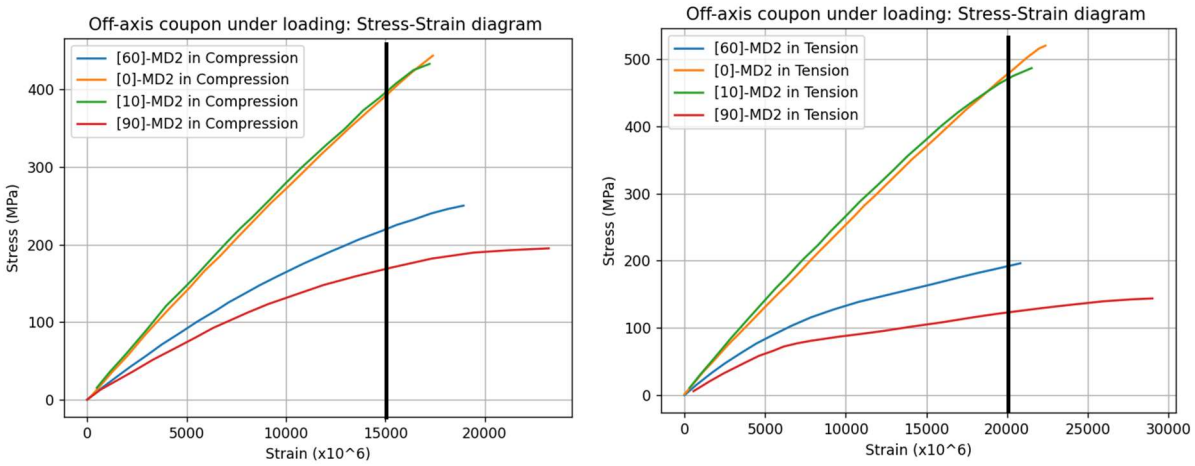

Figure 5-7: Stress-strain diagrams for the experimental results, the black line denotes the strain limit

Continuing down this path of applying a strain limit to the PFA would be outside the scope of this thesis and would make the research unnecessarily lengthy. It is therefore not discussed further.

5.6 Conclusion

The PFA displays promising predictions when combined with the right failure theory and degradation model. Special attention should be paid to the conditions of loading and fiber directions in the laminate when considering how to apply the PFA, as no single failure theory is observed to consistently provide conservative results with low inaccuracy. However, whereas Hashin seems to be more accurate in general, Tsai Hill is more conservative when the laminate is transversely loaded, indicating that Tsai Hill is to be preferred in a design situation when considering a laminate loaded in the weak direction.

PFA provides a good indication of how the multidirectional laminate will behave under a UD load, but an engineer should be aware of when to expect a strengthening behavior between the plies that will boost the capacity of the laminate, and when this behavior will not exist, causing the potential of optimistic results. Furthermore, there is a possibility of reducing the optimistic results by adding a strain limit to the predictions, that do not require much work from the design point of view. However, knowledge of the strain limit to be applied to the laminate is required to be known beforehand. One possibility could be to base the strain limit of the UD experiments, which is approximately 1.5% for 0-C and 2% for 0-T.

6 Multidirectional laminate under biaxial loading

This chapter aims to explore the capabilities of PFA for multidirectional laminates under biaxial loads. Often, failure theories are validated with laminates under UD loads, as was done in the previous chapter. Rarely, is the validation done with biaxial experiments, which can be argued to be more a realistic representation of real-life application, as the loading might appear from a multitude of directions simultaneously. In this chapter, the focus will be on a multidirectional laminate exposed to several biaxial loading ratios. This chapter will start by introducing the cruciform specimen. Thereafter, two uniaxially loaded cruciform specimens will be discussed along with the weakness of the specimens. With this knowledge, the other loading ratios will be discussed. Lastly, recommendations will be made regarding the use of PFA to predict the failure of a multidirectional laminate under biaxial loading conditions. Note that the biaxial experiments have only been performed under tensile loading.

6.1 Introduction to cruciform specimen

The test coupons in OptiMat were made of MD material with a $[\pm 45^o, 0^0]_4[\pm 45^o]$-layup, however, a layer is milled away at each side of the specimen, resulting in a $[[\pm 45^o, 0^0]_2[\pm 45^o]$-layup. Test specimens were delivered by the same company as the coupons in the previous Chapter, LM Glasfiber A/S Denmark. Initially, several different geometries were tested out, before deciding on the geometry shown in Figure 6-1. The test speed is 5kN/minute and is adapted depending on the nine different loading ratios applied to the cruciform specimen. The 0° direction of the fibers is defined to be aligned with the x-axis, whereas the transverse direction of 0° fibers is aligned with the y-axis.

The width of the specimen at the end starts at 25 mm, decreasing to 21.1 mm at the minimum point. At the intersection between the arms, the radius of curvature is 12.5 mm. This smooth decrease of arms results in less load sharing between the arms, as there are less ± 45 fibers to lead the load from one arm to the other, thus, the load is introduced more directly to the test zone of specimen. The test zone is a square with rounded edges with a 6 mm radius and the milled away zone has a tapering of 15^o, see Figure 6-1.

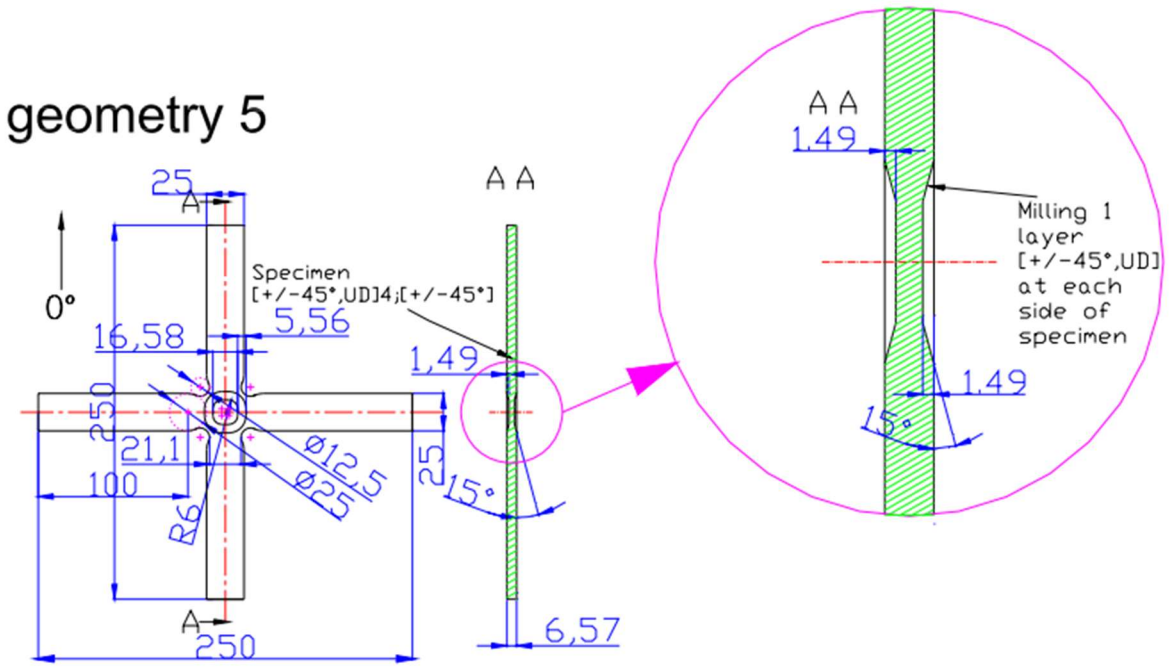

Figure 6-1: Geometry of cruciform specimen used in experiments

There are many variables to consider when experiments are performed on a cruciform specimen, that will influence the experimental results. Therefore, this thesis will limit itself to discussing two points of interest only, the calculation of stress in the test zone, and the influence of the shape of the cruciform specimen. For the application of PFA, it is observed that the strain results for the cruciform specimen are in line with the strains from the beamlike coupons, so the biaxial test results are assumed to be sufficiently valid for the purpose of this thesis. [32]

Table 6-1: Overview of biaxial experiments performed as part of OptiDat scope

Biaxial test specimen - Overview					
Specimen	T or C	Load ratio	Lay-up	Material	Abbreviation
Cruciform	Tension	0/1	$[[\pm 45^o, 0^0]_2[\pm 45^o]$	Combi 1250	0/1-T
Cruciform	Tension	1/0	$[[\pm 45^o, 0^0]_2[\pm 45^o]$	Combi 1250	1/0-T
Cruciform	Tension	0.5/1	$[[\pm 45^o, 0^0]_2[\pm 45^o]$	Combi 1250	0.5/1-T
Cruciform	Tension	0.9625/1	$[[\pm 45^o, 0^0]_2[\pm 45^o]$	Combi 1250	0.9/1-T

Cruciform	Tension	1.925/1	$[[\pm 45^o, 0^0]_2[\pm 45^o]$	Combi 1250	1.9/1-T
Cruciform	Tension	2.567/1	$[[\pm 45^o, 0^0]_2[\pm 45^o]$	Combi 1250	2.5/1-T
Cruciform	Tension	3.85/1	$[[\pm 45^o, 0^0]_2[\pm 45^o]$	Combi 1250	3.8/1-T
Cruciform	Tension	5.775/1	$[[\pm 45^o, 0^0]_2[\pm 45^o]$	Combi 1250	5.7/1-T
Cruciform	Tension	7.7/1	$[[\pm 45^o, 0^0]_2[\pm 45^o]$	Combi 1250	7.7/1-T

Table 6-2: Overview of experimental results on cruciform specimen subject to biaxial loading

Biaxial test specimen – Experimental results				
Experiment*	Axis [y / x]	Fmax [kN]	Stress [MPa]	Strain [%]
0/1-T	X	51	515.58	2.15
	Y	0	0	-1.78
1/0-T	X	0	0	-0.83
	Y	20	138.7	2.16
0.5/1-T	X		100	
	Y		141	
0.9/1-T	X	19	193	
	Y	17	138	
1.9/1-T	X	39	400	
	Y	20	145	
2.5/1-T	X	46	464	
	Y	18	127	
3.8/1-T	X	48	485	
	Y	12	89	
5.7/1-T	X	48	484	
	Y	8	61	
7.7/1-T	X	50	502	
	Y	6	49	

6.2 1/0 and 0/1 loading

Starting with the cruciform under a unidirectional 0/1 and 1/0 loading, the specimens would be expected to behave, and have similar stress, as the beamlike coupons under tensile loading. Note that there are several ways to calculate the stresses, as will be discussed in a later subchapter. The method below was given preference in OptiMat [OB_TG2_R026] and will thus be used when determining the inaccuracy.

Table 6-3: Comparison of unidirectionally loaded MD2 specimen as beamlike and cruciform specimen

UD load in the x-direction						
	Beamlike MD coupons			Cruciform specimen		
	F_x	σ_x	ϵ_x	F_x	σ_x	$\epsilon_x \mid \epsilon_y$
Average	85.2*	519.8	2.24	50.98	515.58	2.15 | -1.78
St.Dev	-	11.5	0.08	3.98	-	0.1 | 0.15
UD load in the y-direction						
	Beamlike MD coupons			Cruciform specimen		
	F_y	σ_y	ϵ_y	F_y	σ_y	$\epsilon_y \mid \epsilon_x$
Average	23.6*	143.9	2.90	19.49	138.7	2.16 | -0.83
St.Dev	-	2.9	0.17		-	0.07 | 0.04

*Derived from stresses by multiplying with nominal area

Table 6-3 compares the beamlike UD-loaded specimen with the biaxially loaded cruciform specimen. The predictions below are not much different from what has already been observed in the previous chapter for the 0- and 90-MDT beamlike coupons under tension. Therefore, there is no need to repeat the discussion at this point.

Table 6-4 Summary of predictions on unidirectionally loaded biaxial coupons

MD2 Cruciform under tension				
Criterion	TD	DNV analytical	RD	Exp.
Tsai Wu	411/0	378/0	428/0	515.58/0
Tsai Hill	411/0	393/0	440/0	
Hashin	411/0	453/0	488/0	
MD2 Cruciform under transverse tension				

Criterion	TD	DNV analytical	RD	Exp.
Tsai Wu	0/59	0/163	0/157	0/143.9
Tsai Hill	0/61	0/165	0/138	
Hashin	0/61	0/163	0/146	

Table 6-5: MD2 cruciform subject to tensile load, in percentage inaccuracy

MD2 Cruciform under tension				
Criterion	TD	DNV analytical	RD	Exp.
Tsai Wu	20% /0	26% /0	17% /0	515.58/0
Tsai Hill	20% /0	23% /0	15% /0	
Hashin	20% /0	12% /0	5% /0	
MD2 Cruciform under transverse tension				
Criterion	TD	DNV analytical	RD	Exp.
Tsai Wu	0 /59%	0 /-13%*	0 /-9%*	0/143.9
Tsai Hill	0 /58%	0 /-15%*	0 /4%*	
Hashin	0 /58%	0 /-13%*	0 /-1%*	

*Optimistic prediction

6.3 Irregularities with cruciform experiments

Issues with the experimental set-up can contest the validity of the test results, or if the test results cannot be transitioned to be applicable to the real world, then calibrating against a fake target would not provide useful insight to be used in the design of structures. Two of these issues will be discussed in this subchapter, as too many detail will not help in answering the main question of the thesis. Rather, the goal is to bring the reader's attention to external factors that can be the cause of the inaccuracy found in the predictions or dispute the value of the results presented in Chapter 6. The issues discussed have been limited to only two influencing factors, and for the purpose of the thesis, an assumption is made that if the biaxial test result is comparable to the UD results, then it is to be considered a valid result [15].

Among the issues mentioned by "Guidelines for biaxial testing of fibre reinforced composites using a cruciform specimen" [16], is an extra compression phenomenon mainly attributed to the geometry of the cruciform specimen and the calculation of stresses. Considering the phenomena related to the extra compression, the strain measurements from the uniaxially loaded cruciform specimen were compared with the strain from uniaxially loaded beamlike coupons.

Table 6-6: Comparison of stress and strain of unidirectionally loaded biaxial coupon

Loading in x-direction				
	Beamlike coupons MD2		Cruciform specimen MD2	
ϵ_x	2.24		2.15	1/0 Load
ϵ_y	-1.11		-1.78	1/0 Load
Loading in y-direction				
ϵ_y	2.90		2.16	0/1 Load
ϵ_x	-		-0.83	0/1 Load

Comparing the two results for uniaxial load in the x.direction, the failure strain for the beamlike coupon is similar to the failure strain of 1/0 loaded cruciform, 2.29 and 2.15 respectively. However, considering the strain in the y-direction as a result of the loading in x-direction, a larger difference is seen between the beamlike and cruciform specimen, 1.11 and 1.78 respectively. The same is true when the loading is applied in the y-direction. These results indicate that extra compressive stress will be present transversely to the tensile loading direction for a cruciform specimen.

To determine the cause of the extra compressive stress, a limited study was performed by “Guidelines for biaxial testing of fibre reinforced composites using a cruciform specimen” [16]. Specimen with different layups were modeled in Abaqus, and the extra compression strain was compared. The study concluded that the extra compression is mainly caused by the cruciform geometry and that the anisotropic nature of GFRP laminates contribute to this effect, depending on the number of transverse fibers causing the load to bypass the central area.

Secondly, there is a need to choose an appropriate method of approximating the stresses, as the load-bearing area is not easily defined, as shown in Figure 6-2. Most failure criteria utilize stress as an input value to determine failure, so the ability to accurately determine the stresses in the biaxial test zone is important for most predictions.

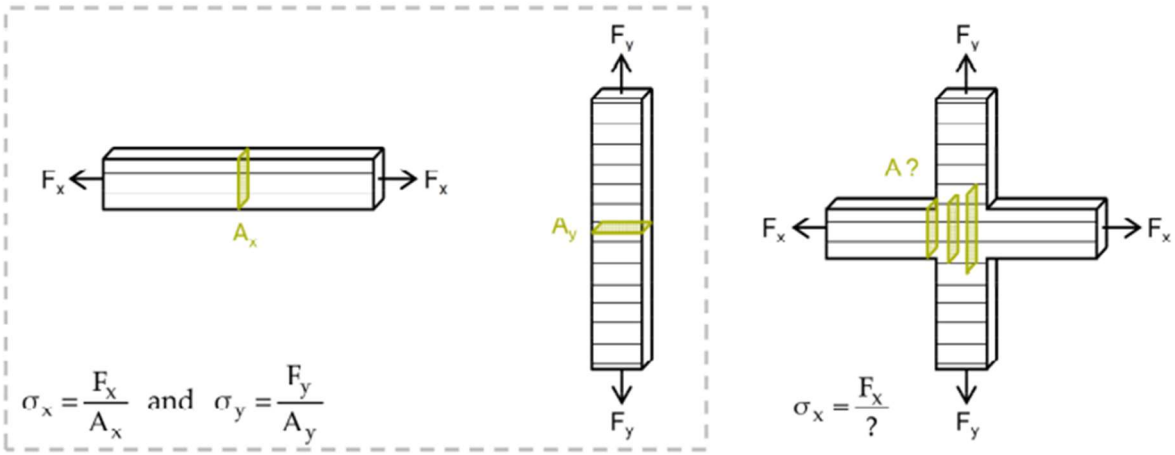

Figure 6-2: Visualization of stress calculations from Guidelines for biaxial testing of FRP using a cruciform specimen

One method, used by OptiDat [16], makes use of an equivalent area assuming failure stresses obtained in the beamlike specimen and uniaxially loaded cruciform specimen will be similar. The second method, described by OptiDat, calculates the failure stresses by using constitutive formulas. The “Guidelines for biaxial testing” consider yet another two methods, Bypass Correction Factor and FE based calculations. Figure 6-3 was produced as part of the comparison between the different methods by C. Ramault [16].

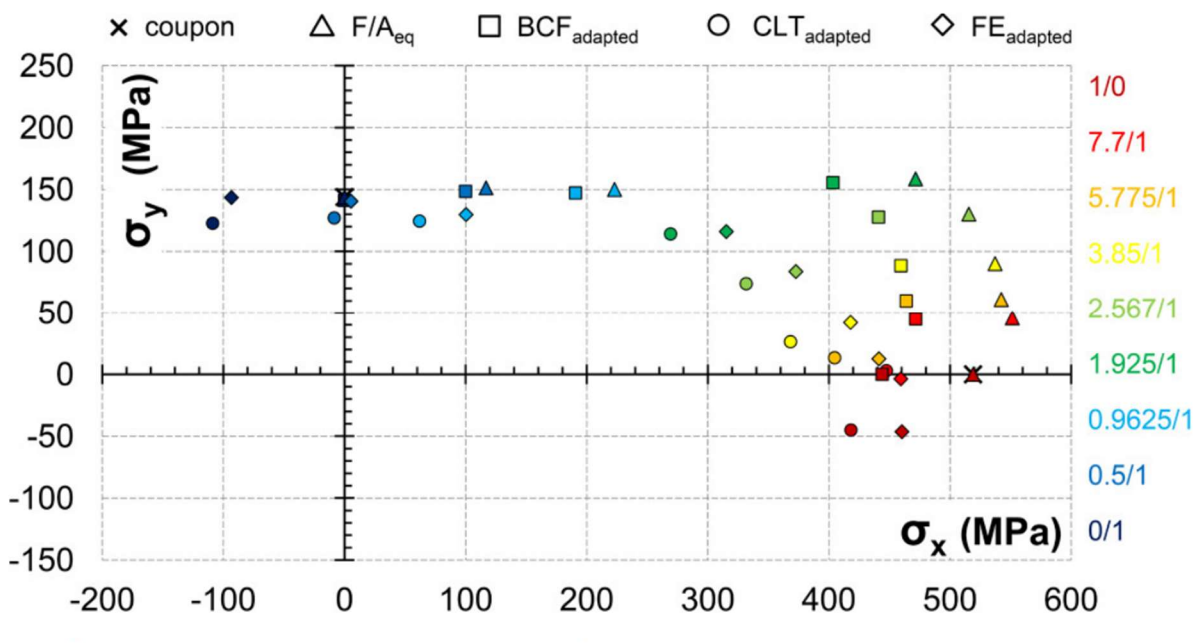

Figure 6-3: A comparison of the methods to calculate the stresses in the central area from "Guidelines for biaxial testing of fibre reinforced composites using a cruciform specimen" [16]

For the purpose of this thesis, the force over an equivalent area method has been utilized, as it was used in the report from OptiDat TG2-025 [16].

6.4 Bi-axial loading ratios

The other 7 loading ratios can be divided into two parts, the loading ratios that are mainly in the y-direction and the main loading in the x-direction. That is: 0,5/1 0,9625/1 as Y-ratios, and 1,925/1, 2,567/1, 3,85/1, 5,775/1, 7,7/1 as X-ratios. Table 6-7 displays the predictions and experimental average for the results with the main loading in the y-direction.

Table 6-7: Summary of predictions with PFA on the Cruciform specimen with main loading ratio in the Y-direction

Criterion	Total Discount	DNV analytical	Residual Discount	Experiment
Cruciform under 0/1 Loading: Y-ratio				
Tsai Wu	0/59	0/163	0/157	0/139
Tsai Hill	0/61	0/165	0/138	
Hashin	0/61	0/163	0/146	
Cruciform under 0.5/1 Loading: Y-ratio				
Tsai Wu	33/66	84/167	83/166	100/141
Tsai Hill	32/65	87/174	70/140	
Hashin	32/65	85/170	76/152	
Cruciform under 0.9625/1 Loading: Y-ratio				
Tsai Wu	70/73	168/174	163/169	193/138
Tsai Hill	63/68	163/169	130/135	
Hashin	65/68	167/174	141/146	

The loading ratio is observed to not be correct for the comparison in Table 6-7. This is due to the approximation done with the equivalent area approximation to convert forces to stresses, as the area is kept constant throughout the conversion based on the area of the beamlike coupons 0-MDT and 90-MDT, whereas a new area should have been considered for each loading ratio. For the load ratio to hold true, the force in the x- and y-direction must be divided by the same area. This makes it very difficult to compare the stresses of the predictions, which are in accordance with the loading ratio, to the experimental stresses. Considering the stresses for 0-5/1-T, Total Discount is always on the conservative side, whereas for Limited discount and Residual discount, the x-direction stresses are conservative, but the y-direction stresses are optimistic. The only exception is Tsai Hill combined with Residual discount, which remains

conservative for stresses in both the x- and y-direction. The same can be repeated for the loading ratio 0.9625/1.

Table 6-8: Summary of predictions on Cruciform specimen with main loading ratio in the Y-direction, in percentage

Criterion	Total Discount	DNV analytical	Residual Discount	Experiment
Cruciform under 0/1 Loading: Y-ratio				
Tsai Wu	0 /59%	0 /-13%	0 /-9%	0/139
Tsai Hill	0 /58%	0 /-15%	0 /1%	
Hashin	0 /58%	0 /-13%	0 /-2%	
Cruciform under 0.5/1 Loading: Y-ratio				
Tsai Wu	67% /53%	16% /-18%	17% /-17%	100/141
Tsai Hill	68% /54%	13% /-23%	30% /1%	
Hashin	68% /54%	15% /-20%	24% /-7%	
Cruciform under 0.9625/1 Loading: Y-ratio				
Tsai Wu	64% /47%	13% /-26%	16% /-22%	193/138
Tsai Hill	67% /50%	16% /-22%	33% /2%	
Hashin	66% /50%	13% /-26%	27% /-6%	

Table 6-8 summarized the Y-ratio predictions in percentages, whereas Table 6-9 shows the summary of X-ratio predictions.

Table 6-9: Summary of PFA predictions on cruciform specimen with main loading ratio in x-direction

Criterion	Total Discount	DNV analytical	Residual Discount	Exp.
Cruciform under 1.925/1 Loading: X-ratio				
Tsai Wu	148/77	343/178	301/156	400/145
Tsai Hill	126/65	325/169	232/120	
Hashin	129/68	335/174	234/122	
Cruciform under 2.567/1 Loading: X-ratio				
Tsai Wu	164/110	437/170	396/154	464/127
Tsai Hill	143/56	431/168	306/119	
Hashin	147/57	443/172	357/139	
Cruciform under 3.85/1 Loading: X-ratio				

Tsai Wu	174/45	512/133	501/130	485/89
Tsai Hill	162/42	513/133	466/121	
Hashin	164/43	512/133	527/137	
Cruciform under 5.775 /1 Loading: X-ratio				
Tsai Wu	184/32	446/77	479/83	484/61
Tsai Hill	165/29	445/77	457/79	
Hashin	173/30	542/78	488/85	
Cruciform under 7.7/1 Loading: X-ratio				
Tsai Wu	239/31	442/58	481/62	502/49
Tsai Hill	183/24	443/58	481/63	
Hashin	203/26	445/58	481/62	
Cruciform under 1/0 Loading: X-ratio				
Tsai Wu	411/0	378/0	428/0	515/0
Tsai Hill	411/0	393/0	440/0	
Hashin	411/0	453/0	488/0	

The Total Discount provides a conservative result for every case. Residual Discount exhibit more accurate and realistic representation of the experiments.

Table 6-10: Summary of PFA predictions on cruciform specimen with main loading ratio in the x-direction, in percentages

Criterion	Total Discount	DNV analytical	Residual Discount	Exp.
Cruciform under 1.925/1 Loading: X-ratio				
Tsai Wu	63% /47%	14% /-22%	24% /-7%	400/145
Tsai Hill	69% /55%	19% /-16%	42% /17%	
Hashin	68% /53%	16% /-20%	41% /15%	
Cruciform under 2.567/1 Loading: X-ratio				
Tsai Wu	65% /13%	6% /-33%	15% / -21%	464/127
Tsai Hill	69% /56%	7% / -32%	34% / 6%	
Hashin	68% /55%	5% /-35%	23% / -9%	
Cruciform under 3.85/1 Loading: X-ratio				
Tsai Wu	64% /49%	-6% /-49%	-3% /-46%	485/89
Tsai Hill	67% /53%	-6% /-49%	4% /-36%	

Hashin	66% /52%	-6% /-49%	-9% /-54%	
Cruciform under 5.775 /1 Loading: X-ratio				
Tsai Wu	61% /48%	8% /-26%	1% /-36%	484/61
Tsai Hill	66% /52%	8% /-28%	6% /-29%	
Hashin	64% /51%	-11% /-28%	-1% /-39%	
Cruciform under 7.7/1 Loading: X-ratio				
Tsai Wu	52% /49%	12% /5%	4% /-2%	502/49
Tsai Hill	63% /61%	12% /5%	4% /3%	
Hashin	59% /57%	11% /5%	4% /-2%	
Cruciform under 1/0 Loading: X-ratio				
Tsai Wu	20% /0	26% /0	17% /0	515/0
Tsai Hill	20% /0	23% /0	15% /0	
Hashin	20% /0	12% /0	5% /0	

Figure 6-4 visualizes all the Residual discount predictions in combination with failure theories. The orange lines show the loading ratios.

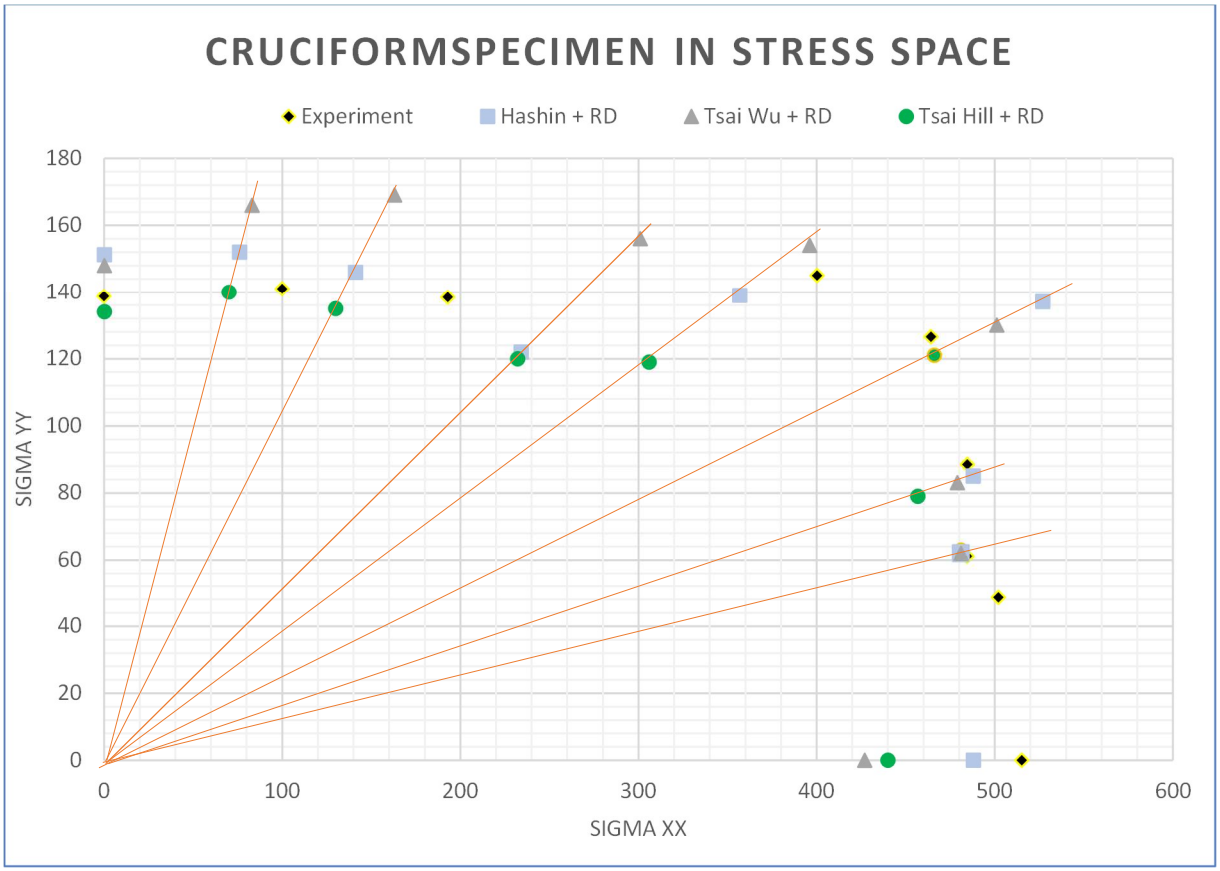

Figure 6-4: Summary of PFA predictions on cruciform specimen in stress space visualized

The visualization in Figure 6-4 clearly show the mismatching loading ratios. However, it is possible to make out trends in the plot. Tsai Wu is observed to be optimistic in many cases, whereas Tsai Hill is seen to be more accurate in addition to conservative. Hashin could be argued to be more precise than Tsai Hill and Tsai Wu, particularly for the X-ratio predictions, even though often optimistic for Y-ratio predictions. To further investigate the results, important statistical parameters are produced and summarized in the Table 6-11:

Table 6-11: Standard deviation and 95% confidence interval for the cruciform specimen, all loading ratios

	MD2 cruciform under tension, Confidence level of 95 %			
	1/0	0/1	0.9625/1	7.7/1
Mean	50.98	19.3	18.7/19.5	49.7/6.5
Std. Dev.	3.98	0.4	0.25/0.24	0.78/0.10
Upper 95% [Force]	57.3	20.6	19.5/20.2	53.0/6.9
Lower 95 % [Force]	44.6	18.1	17.9/18.7	46.3/6.0
Upper 95% [Stress]	580.6	146.7	197.3/143.9	537.3/49.0
Lower 95 % [Stress]	452.4	128.5	181.4/132.9	469.4/43.0
	MD2 cruciform under Tension, Confidence level of 95 %			
	1.925/1	2.567/1	3.85/1	5.775/1
Mean	39.4/20.39	45.8/17.8	48.2/12.5	47.9/8.3
Std. Dev.	0.48/0.29	2.44/0.90	0.55/0.23	2.47/0.44
Upper 95% [Force]	41.5/21.6	51.9/20.0	49.7/13.1	51.9/9.0
Lower 95 % [Force]	37.3/19.2	39.7/15.5	46.6/11.8	44.0/7.6
Upper 95% [Stress]	399.0/145.1	525.5/142.5	503.5/93.4	525.5/63.9
Lower 95 % [Stress]	420.1/153.8	402.7/110.5	472.5/84.2	445.7/54.1

A larger uncertainty in the results can be observed compared to the beamlike coupons, however, this can partly be attributed to the fact that there are fewer test results for the cruciform than there were for the beamlike experiments. This creates a weaker basis for the statistical characterization of the experiments, and also weakens the conclusions that can be drawn.

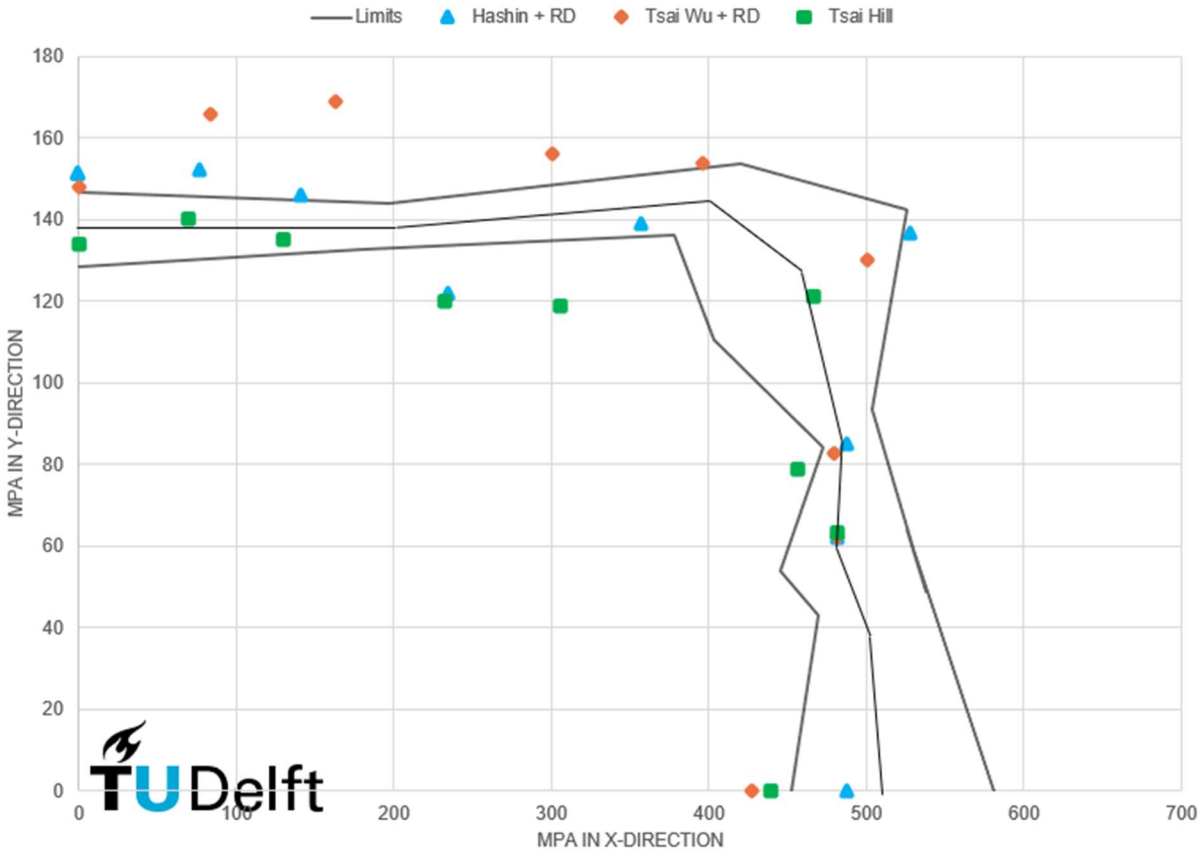

Figure 6-5: Plot of lower and upper 95% confidence level for experimental results and predictions with Residual discount, with three black lines representing the upper, mean, and lower bound.

Figure 6-5 supports the notion that Tsai Hill and Hashin are the two most accurate failure theories, although, Hashin poses a larger risk of being optimistic. Tsai Wu is more often than not, exceeding the mean experimental results. Studying Figure 6-4 and Figure 6-5, it can further be noted that the Y-ratio predictions are consistently overpredicting the stress capacity, which is in line with the observations made in regards to the UD-loaded MD2 beamlike specimen, in which non-conservative predictions were often observed in both the 60-MDT and 90-MDT cases.

Further, it can be argued that there is an upper limit for the loading in both x- and y-directions. Once this limit is exceeded, the laminate will experience failure. This limit can be represented by the mean loading for 1/0 or 0/1 loading ratios. To further confirm this notion of a limit load in the x- and y-direction, it is possible to look at the cruciform test specimen in force-space, which should be a more true representation of the laminate failure points.

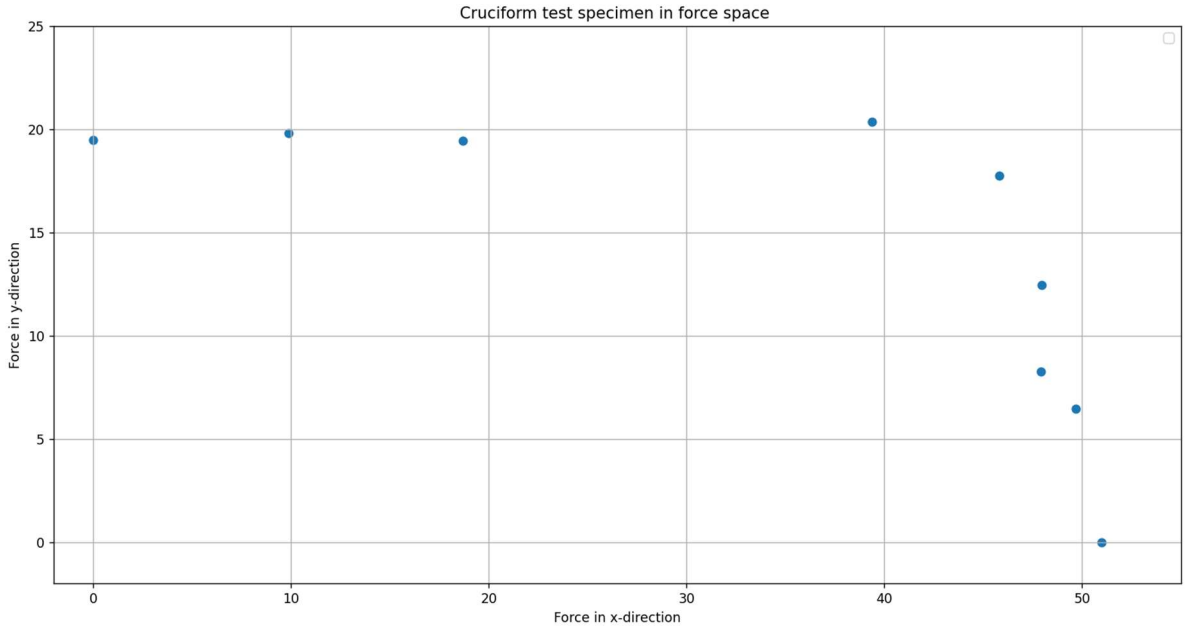

Figure 6-6 Experimental results of cruciform specimen in force-space

6.5 Conclusion

The PFA can indicate the failure of a laminate under bi-axial loading conditions. However, the conversion of the bi-axial experimental results to stress-space is not straight forward and represents an uncertainty with regards to the validity of a direct comparison between the experiment and prediction because of the mismatch in the loading ratio.

With this in mind, Tsai Hill seems to be the most appropriate failure theorem for use in a design situation among the considered criteria, as it only exceeds the mean value twice in predicting the failure. In 4 of the 9 cases, Tsai Hill is conservative when compared to the 95^{th} percentile lower bound, and below mean in another 3 cases. Hashin shows itself to be more useful when the prediction is mainly in the x-direction, i.e. the fiber-dominated direction, as it is less conservative than Tsai Hill. Whereas in the y-direction, although accurate, there is a larger risk of optimistic results when compared to the experiments. Tsai Wu should not be used with Residual discount, particularly in the weak direction of the laminate, as it is often seen to exceed the upper bound of the 95^{th} percentile.

7 Conclusions and recommendations

7.1 Conclusions

This study seeks to develop a deeper understanding of how GFRP laminates behave when subject to static loading conditions under multiaxial stress states by the application of PFA as outlined in the technical specification, CEN TS19101. The PFA utilizes a 5-step approach, which involves incorporating the CLT, failure theories, and degradation models to estimate the failure of individual layers within the GFRP laminate until final failure is reached. The conclusion chapter will consider the MD2 laminate, [(45/-45/0)4 / 45/-45], subject to UD and biaxial loading in combination with the Total Discount (subquestion 1) and Residual Discount (subquestion 2) degradation models, see Chapter 3.4 for more details regarding the cases considered. First, the three subquestions will be answered:

1. *How inaccurate is the method specified in the TS19101 Annex B.8 in predicting the final failure of a GFRP laminate under static loading?*
   - Considering the MD2 beamlike coupons subject to a UD tensile load, an average inaccuracy of 48% is anticipated. The outcome is conservative in each individual prediction. For a comprehensive explanation, see Chapters 5.2, 5.3, and 5.4.
   - In the case of compression on UD-loaded MD2 beamlike coupons, an average inaccuracy of 29% is expected, with each prediction being a conservative estimate. For a more thorough analysis, see Chapters 5.2, 5.3, and 5.4.
   - Evaluating the biaxially loaded MD2 cruciform specimen, an inaccuracy of 55% can be expected on average. See Chapter 6.2 and 6.4 for more details.
2. *Considering the cause of the inaccuracy exposed in the initial predictions, how can the predictions of PFA be improved to better represent the laminate behavior?*
   - The inaccuracy observed can be attributed to two factors: Firstly: The Total degradation model imposes an overly severe penalty on the failed plies. Secondly, the choice of failure theory does not always differentiate between failure modes, thus, Total Degradation is applied. However, by implementing the Residual Discount degradation model and failure indices, both issues are addressed and a significant reduction of inaccuracy can be achieved.
   - When analyzing the UD-loaded MD2 beamlike specimens subject to tension, an inaccuracy of 14% is anticipated, with some predictions being optimistic. For more detailed findings, see Chapter 5.5.

- When examining UD-loaded MD2 beamlike specimens subject to compression, an inaccuracy of 24% is anticipated, also with some optimistic results. For more details, see Chapter 5.5.
- Considering biaxially loaded MD2 specimen, an average inaccuracy of 16% can be expected, with both conservative and optimistic predictions. See Chapter 6.2 and 6.4 for a detailed answer.

3. *What recommendations might be given to engineers considering time and effort used in making the predictions, compared to the level of accuracy achieved?*
   - Engineers can be confident that employing the **Total Discount model will produce conservative results** while being **easy to apply**.
   - The **Residual Discount model provides the most accurate predictions**. However, **additional time** is required to select an appropriate Residual Discount mode, failure criterion and constraints such as strain limit to ensure conservatism.

Main question:

"What is the inaccuracy by which the final ply failure of in-plane dominated Glass Fibre-Reinforced Polymer laminates under multi-axial stress states can be predicted by progressive failure analysis as described in TS19101, based on existing knowledge and experimental results?"

This study demonstrates the application of PFA as outlined in TS19101 to predict the failure of a multidirectional GFRP laminate under UD and biaxial loading conditions. The accuracy of the predictions is greatly influenced by the choice of degradation model and failure theory, ranging from approximately 1% to 70%, highlighting the importance of selecting an appropriate degradation model and failure criterion. The largest inaccuracy is found with Total Discount, as responded to subquestion 1, however, this inaccuracy can be greatly reduced by the use of existing knowledge to better represent GFRP laminate behavior to predict the final failure of a laminate, as is shown in the answer to subquestion 2. Specifically, in this research, the application of a residual discount model reduces the inaccuracy by 19 and 39 percentage points for the MD2 specimen subjected to uniaxial and biaxial loading, respectively, compared to the Total Discount degradation model.

7.2 Recommendations

This subchapter will be structured into two sections, each offering recommendations pertaining to various aspects relevant to this thesis.

Recommendation regarding use of Progressive Failure Analysis

- **Total Discount** is a severe model of degradation, which ensures highly conservative result in every case that has been considered in this research. An engineer can be confident that a design in which Total Discount model is combined with any failure theory of choice, will yield residual laminate strength compared to reality. This conclusion can be extended to an arbitrary laminate configuration loaded in any random direction, indicating that Total Discount **is likely to result in a conservative outcome**.
- **The Limited Discount** model can be considered as an intermediate option between Total and Residual Discount models in terms of accuracy achieved. Nonetheless, caution should be adopted when employing this model, as optimistic predictions have been observed in specific instances. Therefore, engineers incorporating the Limited Discount model in their calculations should **be mindful of how the model influences the redistribution of individual ply stresses following FPF**. Based on the findings of this thesis, the **Limited Discount model is recommended to be combined with the Hashin failure theory**. Furthermore, itis **most suitable for scenarios involving tension, where at least 50% of the fibers are aligned with the load direction.**
- **The Residual discount model** provides the most accurate predictions on average. While there are some instances of optimistic predictions, **engineers can rely on the residual discount model to offer a realistic indication of the laminate's behavior** until FPF. For optimal use in civil engineering applications, the **selection of an appropriate failure theory significantly influences the ability to achieve conservative predictions.**
- In scenarios where the prediction pertains to tensile or compressive loading when at least 50% of the fibers are aligned in the loading direction, Hashin criterion proves to be the most accurate choice in addition to being conservative. However, when the laminate is subjected to loading in the weak direction, particularly under compressive loading, the Hashin criterion tends to overestimate the stress capacity. In such cases, the **Tsai Hill failure criterion is more suitable for ensuring conservative predictions**.

- The biaxially loaded cruciform specimen visualizes how the predictions turn from being conservative on average when the specimen is loaded mainly in the strong x-direction along the fibers, to lean towards overpredicting the stress capacity when loaded mainly in the weak y-direction transverse to the fibers.

Recommendations regarding limitations of Progressive Failure Analysis

- Only a single laminate lay-up has been considered in this research. However, by expanding the range of lay-ups under consideration, greater confidence could be instilled in the conclusions reached.
- A more gradual reduction of the material properties can increase the accuracy and conservatism achieved by Residual. However, within the scope of which PFA is supposed to be used, a simplification would be more convenient in terms of speed versus accuracy.
- Strain limit shows potential in limiting the cases in which the predictions end up being optimistic. If the strain limit of an arbitrarily built laminate is known beforehand, this would be easy to implement. However, this is seldom the case.
- More failure theories, such as Puck, should be included to evaluate the inaccuracy. Some failure theories work better under certain conditions, knowing the optimal conditions for the use of a criterion would help with the accuracy of predictions.
- When considering the implementation of the residual discount model, designers must determine the extent to which each stiffness parameter should be reduced in the event of matrix failure. This decision can be based on available literature or be developed based on experimental procedure outlined in DNV ST-C501. More effort should be put into developing a residual degradation model fit for use in different cases, as the choice of degradation model greatly affects the predictions.

References

[1] F. Paris and G. Washington, “A Study of Failure Criteria of Fibrous Composite Materials,” 2001. [Online]. Available: http://www.sti.nasa.gov

[2] P. D. Soden, A. S. Kaddour, and M. J. Hinton, “Recommendations for designers and researchers resulting from the world-wide failure exercise,” *Compos Sci Technol*, vol. 64, no. 3–4, pp. 589–604, 2004, doi: 10.1016/S0266-3538(03)00228-8.

[3] L. Ascione, “TOWARDS A STRUCTURAL EUROCODE FOR FRP STRUCTURES: THE ROLE OF CEN/TC 250,” 2018. [Online]. Available: https://www.researchgate.net/publication/326551681

[4] J. Clarke, “Structural Design of Polymer Composites,” 2005.

[5] J. Montesano and C. V. Singh, “Critical stiffness damage envelopes for multidirectional laminated structures under multiaxial loading conditions,” *Mater Des*, vol. 91, pp. 218–229, Feb. 2016, doi: 10.1016/j.matdes.2015.11.110.

[6] S. Li *et al.*, “Damage related material constants in continuum damage mechanics for unidirectional composites with matrix cracks,” *International Journal of Damage Mechanics*, vol. 28, no. 5, pp. 690–707, Jun. 2018, doi: 10.1177/1056789518783239.

[7] George. Lubin and S. T. (Stanley T.) Peters, *Handbook of composites*. Chapman & Hall, 1998.

[8] DNV, “DNV-ST-C501 Composite components,” 2022.

[9] T. A. Bogetti, C. P. R. Hoppel, V. M. Harik, J. F. Newill, and B. P. Burns, “Predicting the nonlinear response and failure of composite laminates: Correlation with experimental results,” 2004.

[10] S. S. R. Koloor, “SIMULATION METHODOLOGY FOR FRACTURE PROCESSES OF COMPOSITE LAMINATES USING DAMAGE-BASED MODELS,” 2016.

[11] J. Montesano and C. V. Singh, “Stiffness Critical Damage Envelopes for Multidirectional Composite Laminates Under Multiaxial Loading Conditions,” 2015. [Online]. Available: https://www.researchgate.net/publication/280721878

[12] A. M. Van Wingerde and Delft D R V Van, “Input data for a comparison between uni-axial and bi-axial stresses OB_TG2_R015,” 2004.

[13] L. J. Hart-Smith, “Comparison between theories and test data concerning the strength of various fibre-polymer composites,” 2004.

[14] M. Hinton, P. Soden, and A. Kaddour, “Preface_2004_Failure-Criteria-in-Fibre-Reinforced-Polymer-Composites”.

[15] M. J. Hinton, A. S. Kaddour, and P. D. Soden, “The world-wide failure exercise: Its origin, concept and content,” 2004.

[16] C. Ramault, “Guidelines for biaxial fibre reinforced a cruciform specimen,” 2012.

[17] L. G. J. Janssen *et al.*, “Final Report: Reliable Optimal Use of Materials for Wind Turbine Rotor Blades OB_PC_R017 rev. 001,” 2001.

[18] T. P. Philippidis, A. E. Antoniou, V. Passipoularidis, and T. T. Assimakopoulou, “Static Tests On the Standard OB Unidirectional Coupon OB_TG2_R018,” 2004.

[19] T. P. Philippidis, A. E. Antoniou, T. T. Assimakopoulou, and V. A. Passipoularidis, “Static Tests on the Standard OB UD and MD off-axis Coupons OB_TG2_R022,” 2005.

[20] M. A. Muflikhun and B. Fiedler, “Failure Prediction and Surface Characterization of GFRP Laminates: A Study of Stepwise Loading,” *Polymers (Basel)*, vol. 14, no. 20, Oct. 2022, doi: 10.3390/polym14204322.

[21] G. C. Eckold, “Failure criteria for use in the design environment,” 2004.

[22] P. K. Gotsis, C. C. Chamis, and L. Minnetyan, “Application of progressive fracture analysis for predicting failure envelopes and stress-strain behaviors of composite laminates: a comparison with experimental results,” 2004.

[23] T. P. Philippidis, A. P. Vassilopoulos, T. T. Assimakopoulou, and V. Passipoularidis, “Static and Fatigue Tests of OPTIMAT UD coupons. OB_TG2_R012,” 2003.

[24] T. Philippidis, “Test program for basic material (UD plate) characterization,” 2002.

[25] T. P. Philippidis, “Verification test program. UD off-axis and MD specimens OB_TG2_004,” 2002.

[26] G. Kress, “Examination of Hashin’s failure criteria for the second world-wide failure exercise,” *J Compos Mater*, vol. 46, no. 19–20, pp. 2539–2561, Sep. 2012, doi: 10.1177/0021998312449892.

[27] A. Kuraishi, S. W. Tsai, and K. K. S. Liu, “A progressive quadratic failure criterion, part B,” 2004.

[28] Y. Guo-qing, R. Yi-ru, Z. Tian-tian, X. Wan-shen, and J. Hong-yong, “Hashin Failure Theory Based Damage Assessment Methodology of Composite Tidal Turbine Blades and Implications for the Blade Design,” 2018, doi: 10.1007/s13344-018.

[29] Z. Hashin, “Failure Criteria for Unidirectional Fiber Composites 1,” 1980. [Online]. Available: http://www.asme.org/about-asme/terms-of-use

[30] L. Kroll and W. Hufenbach, “Physically Based Failure Criterion for Dimensioning of Thick-Walled Laminates,” Kluwer Academic Publishers, 1997.

[31] M. Koetsier, “Virtual fatigue verification of Glass Fibre-Reinforced Polymer components for civil engineering applications,” 2021. [Online]. Available: http://repository.tudelft.nl/.

[32] A. Smits and D. Van Hemelrijck, “Biaxial test results on cruciform specimens OB_TG2_R026,” 2005.

Appendix I

Table A-I 1Summary of in-plane mechanical properties from OPTIMAT UD material based on experimental results in GPA

Statistics	E1	E2	E2	E2c	G12	V12	V21
Min	36.64	37.44	13.54	14.41	4.032	0.24	0.0836
Max	41.38	40.1	14.73	15.65	4.396	0.3459	0.0950
Std. Dev	1.0323	0.5820	0.3248	0.2549	0.00992	0.0271	0.0065
Obs.	29	26	25	26	24	29	25
Mean	29.042	38.865	14.077	14.998	4.239	0.291	0.095

Table A-I 2: Summary of in-plane mechanical strength properties from OPTIMAT UD material based on experimental results in GPA

Statistics	X	X’	Y	Y’	S
Min	695.0	-541.6	49.6	-171.7	54.0
Max	836.0	-480.8	59.9	-149.0	57.8
Std. Dev	36.143	16.500	2.576	4.849	1.119
Obs.	29	26	25	26	25
Mean	776.5	-521.8	54.0	-165.0	56.1

Appendix II: Predictions, detailed results

First, the UD coupons, then the MD2 coupons, and finally the cruciform predictions.

0- and 90- degree UD coupon under tension and compression:

Table A-II a: Summary of experiment on UD on-axis specimen compared to predictions

Unidirectional coupons					
	Experimental results		Predicted results		Difference Stress|Strain
Coupon	Stress [MPa]	Strain [%]	Predicted Stress [MPa]	Predicted Strain [%]	Difference Stress|Strain
[0] Tension	776.50	2.091	776.5	1.9895	0 % | 5 %
[0] Compr.	-525.91	-1.417	-521.9	-1.3367	1 % | 6 %
[90] Tension	53.95	0.422	53.9	0.383	0 % | 10 %
[90] Compr.	-165.02	-1.9975	-165	-1.1728	0 % | 70 %

10 degree UD coupon under tension:

Table A-II b 10-T laminate, detailed predictions with Tsai Wu

Tsai Wu Criterion	Degradation model with failure indices on [10] coupon, tension			
Initial failure prediction, axial stress and strain				
Degradation model	Total discount	Limited discount, TS	Limited discount, DNV	Residual Discount
Stress [MPa]	308.60	--	--	--
Strain [%]	0.009453	--	--	--
Final failure prediction, axial stress and strain				
Stress [MPa]	--	--	--	--
Strain [%]	--	--	--	--

Table A-II c 10-T laminate, detailed predictions with Tsai Hill

Tsai Hill Criterion	Degradation model with failure indices on [10] coupon, tension			
Initial failure prediction, axial stress and strain				
Degradation model	Total discount	Limited discount, TS	Limited discount, DNV	Residual Discount
Stress [MPa]	300	--	--	--
Strain [%]	0.009189	--	--	--
Final failure prediction, axial stress and strain				
Stress [MPa]	--	--	--	--
Strain [%]	--	--	--	--

Table A-II d 10-T laminate, detailed predictions with Hashin

Hashin Criterion	Degradation models on [10] coupon, tension			
Initial failure prediction, axial stress and strain				
Degradation model	Total discount	Limited discount, TS	Limited discount, DNV	Residual Discount
Stress [MPa]	303.57	--	--	--
Strain [%]	0.009229	--	--	--
Final failure prediction, axial stress and strain				
Stress [MPa]	--	--	--	--
Strain [%]	--	--	--	--

10 degree UD coupon under Compression.

Table A-II e 10-C laminate, detailed predictions with Tsai Wu

Tsai Wu Criterion	Degradation models, on [10] coupon, Compression			
Initial failure prediction, axial stress and strain				
Degradation model	Total discount	Limited discount, TS	Limited discount, DNV	Stephen Tsai method
Stress [MPa]	289.12	--	--	--
Strain [%]	0.008856	--	--	--
Final failure prediction, axial stress and strain				
Stress [MPa]	--	--	--	289.12
Strain [%]	--	--	--	0.012678*

*Strain after failure

Table A-II f 10-C laminate, detailed predictions with Tsai Hill

Tsai Hill Criterion	Degradation models, on [10] coupon, Compression			
Initial failure prediction, axial stress and strain				
Degradation model	Total discount	Limited discount, TS	Limited discount, DNV	Stephen Tsai method
Stress [MPa]	281.49	--	--	--
Strain [%]	0.008622	--	--	--
Final failure prediction, axial stress and strain				

Stress [MPa]	--	--	--	281.49
Strain [%]	--	--	--	0.012343

*Stain after failure

Table A-II g 10-C laminate, detailed predictions with Hashin

Hashin Criterion	Degradation models, on [10] coupon, Compression			
Initial failure prediction, axial stress and strain				
Degradation model	Total discount	Limited discount, TS	Limited discount, DNV	Stephen Tsai method
Stress [MPa] MF	338.47	--	--	--
Strain [%] MF	0.010368	--	--	--
Final failure prediction, axial stress and strain				
Stress [MPa]	--	--	--	338.47
Strain [%]	--	--	--	0.014842*

* Stain after failure

60 degree UD coupon under tension

Table A-II h 60-T laminate, detailed predictions with Tsai Wu

Tsai Wu Criterion	Degradation models, on [60] coupon, Tension			
Initial failure prediction, axial stress and strain				
Degradation model	Total discount	Limited discount, TS	Limited discount, DNV	Stephen Tsai method
Stress [MPa]	60.75	--	--	--
Strain [%]	0.005046	--	--	--
Final failure prediction, axial stress and strain				
Stress [MPa]	--	--	--	60.75
Strain [%]	--	--	--	0.013509*

* Stain after failure

Table A-II i 60-T laminate, detailed predictions with Tsai Hill

Tsai Hill Criterion	Degradation models, on [60] coupon, Tension			
Initial failure prediction, axial stress and strain				
Degradation model	Total discount	Limited discount, TS	Limited discount, DNV	Stephen Tsai method
Stress [MPa]	63.0	--	--	--
Strain [%]	0.005232	--	--	--
Final failure prediction, axial stress and strain				
Stress [MPa]	--	--	--	63.0
Strain [%]	--	--	--	0.014001*

* Stain after failure

Table A-II j 60-T laminate, detailed predictions with Hashin

Hashin Criterion	Degradation models, on [60] coupon, Tension			
Initial failure prediction, axial stress and strain				
Degradation model	Total discount	Limited discount, TS	Limited discount, DNV	Stephen Tsai method
Stress [MPa] MF	63.0	--	--	--

Strain [%] MF	0.005232	--	--	--
Final failure prediction, axial stress and strain				
Stress [MPa]	--	--	--	63
Strain [%]	--	--	--	0.014001*

*Strain after failure

60 degree UD coupon under compression

Table A-II k 60-C laminate, detailed predictions with Tsai Wu

Tsai Wu Criterion	Degradation models, on [60] coupon, Compression			
Initial failure prediction, axial stress and strain				
Degradation model	Total discount	Limited discount, TS	Limited discount, DNV	Stephen Tsai method
Stress [MPa]	137.5	--	--	--
Strain [%]	0.011422	--	--	--
Final failure prediction, axial stress and strain				
Stress [MPa]	--	--	--	137.5
Strain [%]	--	--	--	0.029475*

*Strain after failure

Table A-II l 60-C laminate, detailed predictions with Tsai Hill

Tsai Hill Criterion	Degradation models, on [60] coupon, Tension			
Initial failure prediction, axial stress and strain				
Degradation model	Total discount	Limited discount, TS	Limited discount, DNV	Stephen Tsai method
Stress [MPa]	112.01	--	--	--
Strain [%]	0.009305	--	--	--
Final failure prediction, axial stress and strain				
Stress [MPa]	--	--	--	112.01
Strain [%]	--	--	--	0.024211*

*Strain after failure

Table A-II m 60-C laminate, detailed predictions with Hashin

Hashin Criterion	Degradation models, on [10] coupon, Tension			
Initial failure prediction, axial stress and strain				
Degradation model	Total discount	Limited discount, TS	Limited discount, DNV	Stephen Tsai method
Stress [MPa] MF	126.62	--	--	--

Strain [%] MF	0.010519	--	--	--
Final failure prediction, axial stress and strain				
Stress [MPa]	--	--	--	126.62
Strain [%]	--	--	--	0.027369*

*Strain after failure

0-degree MD2 coupon under compression

Table A-II n 0-MDC laminate, detailed predictions with Tsai Wu

Tsai Wu Criterion	Model of degradation combined with failure indices			
Initial failure prediction, 0 plies FF				
Degradation model	Total discount	Limited discount, TS	DNV Analytical	Residual property
Stress [MPa]	257.82	--	--	--
Strain [%]	0.009596	--	--	--
Final failure prediction, axial stress and strain, 45 plies				
Stress [MPa]	60.47	60.47	→ 70.94	56.78
Strain [%]	0.009596	0.009596	→26.23	0.022893

Table A-II o 0-MDC laminate, detailed predictions with Tsai Hill

Tsai Hill Criterion	Model of degradation combined with failure indices			
Initial failure prediction, axial stress and strain, 45 plies				
Degradation model	Total discount	Limited discount, TS	DNV Analytical	Residual property
Stress [MPa] [45]	236.87	--	--	--
Strain [%]	0.008696	--	--	--
Final failure prediction, axial stress and strain, 0 plies				
Stress [MPa]	277.43	211.8	211.8	251.03
Strain [%]	0.013472	0.009612	0.009612	0.010517

Table A-II p 0-MDC laminate, detailed predictions with Hashin

Hashin Criterion	Model of degradation combined with failure indices			
Degradation model	Total discount	Limited discount, TS	DNV analytical	Residual property
Initial failure prediction: MF compression of 45-plies – 267.7 N/mm^2 – 0.9827%				
Final failure prediction, axial stress and strain – 0 Plies				
Stress [MPa]	277.43	305.6	305.6	329.2
Strain [%]	0.013472	0.013869	0.013869	0.013789

Mode – 0 plies	Fiber T	Fiber T	Fiber T	Fiber T

0-degree MD2 coupon under tension

Table A-II q 0-MDT laminate, detailed predictions with Tsai Wu

Tsai Wu Criterion	Model of degradation combined with failure indices			
Initial failure prediction, axial stress and strain				
Degradation model	Total discount	Limited discount, TS	DNV analytical	Residual property
Stress [MPa]	182.59	--	--	--
Strain [%]	0.006686	--	--	--
Final failure prediction, axial stress and strain				
Stress [MPa]	411.46	378.00	377.00	427.68
Strain [%]	0.019893	0.017083	0.017083	0.017857

Table A-II r 0-MDT laminate, detailed predictions with Tsai Hill

Tsai Hill Criterion	Model of degradation combined with failure indices			
Initial failure prediction, axial stress and strain				
Degradation model	Total discount	Limited discount, TS	DNV analytical	Residual property (RD)
Stress [MPa] [45]	189.14	--	--	--
Strain [%]	0.006926	--	--	--
Final failure prediction, axial stress and strain				
Stress [MPa]	411.46	393.60	393.60	439.88
Strain [%]	0.019889	0.017769	0.017769	0.018366

Table A-II s 0-MDT laminate, detailed predictions with Hashin

Hashin Criterion	Model of degradation combined with failure indices			
Initial failure prediction, axial stress and strain				
Degradation model	Total discount	Limited discount, TS	DNV analytical	Residual property

Stress [MPa] [45]	189.88	--	--	--
Strain [%]	0.006953	--	--	--
Mode – 45 plies	Matrix T	Matrix T	Matrix T	Matrix T
Final failure prediction, axial stress and strain				
Stress [MPa]	411.30	452.98	452.98	487.65
Strain [%]	0.019893	0.020473	0.020473	0.020361
Mode – 0 plies	Fiber T	Fiber T	Fiber T	Fiber T

60-degree MD laminate under tension

Table A-II t 60-MDT laminate, detailed predictions with Tsai Wu

Tsai Wu Criterion	Model of degradation combined with failure indices			
Initial failure prediction, axial stress and strain – 75 plies – Fiber failure				
Degradation model	Total discount	Limited discount, TS	Limited discount, DNV	Stephen Tsai method
Stress [MPa]	78.8	--	--	--
Strain [%]	0.004384	--	--	--
Secondary failure prediction, axial stress and strain – 60 plies				
Stress [MPa]	69.2	67.4	67.4	72.8
Strain [%]	0.004716	0.004544	0.004544	0.004494
Final failure prediction+ , axial stress and strain - 10 plies				
Stress [MPa]	53.5	75.1	75.1	139.1
Strain [%]	0.00807	0.01002	0.01002	0.011531

*Optimistic result

Table A-II u 60-MDT laminate, detailed predictions with Tsai Hill

Tsai Hill Criterion	Model of degradation combined with failure indices			
Initial failure prediction, axial stress and strain – 55 plies				
Degradation model	Total discount	Limited discount, TS	Limited discount, DNV	Stephen Tsai method
Stress [MPa]	525	--	--	--
Strain [%]	0.004496	--	--	--
Secondary failure prediction, axial stress and strain – 35 plies				
Stress [MPa]				
Strain [%]				
Final failure prediction, axial stress and strain - 10 plies				
Stress [MPa]				
Strain [%]				

*Optimistic result

Table A-II v 60-MDT laminate, detailed predictions with Hashin

Hashin Criterion	Model of degradation combined with failure indices			
Initial failure prediction, axial stress and strain – 75 plies				
Degradation model	Total discount	Limited discount, TS	Limited discount, DNV	Stephen Tsai method
Stress [MPa]	525	--	--	--
Strain [%]	0.004496	--	--	--
Secondary failure prediction, axial stress and strain – 60 plies				
Stress [MPa]	462	450	450	482
Strain [%]	0.004841	0.004669	0.004669	0.00458
Final failure prediction, axial stress and strain - 15 plies				
Stress [MPa]				967
Strain [%]				0.012335
Final failure prediction, axial stress and strain - 15 plies				
				1609
				0.021875
Improvement and difference in result compared to Base result				

*Optimistic result

10 degree MD2 laminate in tension

Table A-II w 10-MDT laminate, detailed predictions with Tsai Wu

Tsai Wu Criterion	Model of degradation combined with failure indices			
Initial failure prediction, axial stress and strain – 55 plies				
Degradation model	Total discount	Limited discount, TS	Limited discount, DNV	Stephen Tsai method
Stress [MPa]	141.69	141.69	141.69	141.69
Strain [%]	0.005259	0.005259	0.005259	0.005259
Secondary failure prediction, axial stress and strain – 35 plies				
Stress [MPa]	227.08	224	224	230.15
Strain [%]	0.009416	0.009279	0.009279	0.00911
Final failure prediction, axial stress and strain - 10 plies				
Stress [MPa]	166.31	357.08	357.08	394.31
Strain [%]	0.00946	0.016018	0.016018	0.016413

*Optimistic result

Table A-II x10-MDT laminate, detailed predictions with Tsai Hill

Tsai Hill Criterion	Model of degradation combined with failure indices			
Initial failure prediction, axial stress and strain – 55 plies				
Degradation model	Total discount	Limited discount, TS	Limited discount, DNV	Stephen Tsai method
Stress [MPa]	149.1	149.1	149.1	149.1
Strain [%]	0.005533	0.005533	0.005533	0.005533
Secondary failure prediction, axial stress and strain – 35 plies				
Stress [MPa]	227.1	227.1	227.1	227.1
Strain [%]	0.009416	0.00933	0.00933	0.009164
Final failure prediction, axial stress and strain - 10 plies				
Stress [MPa]	164.5	339.6	339.7	373.4
Strain [%]	0.009189	0.015238	0.015238	0.015542

*Optimistic result

Table A-II y 10-MDT laminate, detailed predictions with Hashin

Hashin Criterion	Model of degradation combined with failure indices

Initial failure prediction, axial stress and strain – 55 plies				
Degradation model	Total discount	Limited discount, TS	Limited discount, DNV	Stephen Tsai method
Stress [MPa]	149.1			
Strain [%]	0.005533			
Secondary failure prediction, axial stress and strain – 35 plies				
Stress [MPa]	235.4	235.4	235.4	238.7
Strain [%]	0.009761	0.009751	0.009751	0.009457
Final failure prediction, axial stress and strain - 10 plies				
Stress [MPa]	163.5	361.5	361.5	389.2
Strain [%]	0.009303	0.016218	0.016218	0.016202

*Optimistic result

10 degree MD2 laminate under compression

Table A-II z 10-MDC laminate, detailed predictions with Tsai Wu

Tsai Wu Criterion	Model of degradation combined with failure indices			
Initial failure prediction, axial stress and strain – 10 plies – Fiber failure				
Degradation model	Total discount	Limited discount, TS	Limited discount, DNV	Stephen Tsai method
Stress [MPa]	-265.8	-265.8	-265.8	-265.8
Strain [%]	-0.009866	-0.009866	-0.009866	-0.009866
Secondary failure prediction, axial stress and strain – 35 plies				
Stress [MPa]	N/A	N/A	N/A	N/A
Strain [%]	N/A	N/A	N/A	N/A
Final failure prediction, axial stress and strain - 10 plies				
Stress [MPa]	N/A	N/A	N/A	N/A
Strain [%]	N/A	N/A	N/A	N/A

*Optimistic result

Table A-II aa 10-MDC laminate, detailed predictions with Tsai Hill

Tsai Hill Criterion	Model of degradation combined with failure indices			
Initial failure prediction, axial stress and strain – 55 plies				
Degradation model	Total discount	Limited discount, TS	Limited discount, DNV	Stephen Tsai method
Stress [MPa]	244.2	--	--	--
Strain [%]	0.009061	--	--	--
Secondary failure prediction, axial stress and strain – 35 plies				
Stress [MPa]	226.2	227.5	227.5	235.5
Strain [%]	-0.009384	-0.009426	-0.009426	-0.009335
Final failure prediction, axial stress and strain - 10 plies				
Stress [MPa]	151.7	232.6	232.6	263.8
Strain [%]	-0.008629	-0.010435	-0.010435	-0.010983

*Optimistic result

Table A-II bb 10-MDC laminate, detailed predictions with Hashin

Hashin Criterion	Model of degradation combined with failure indices
Initial failure prediction, axial stress and strain – 55 plies	

Degradation model	Total discount	Limited discount, TS	Limited discount, DNV	Stephen Tsai method
Stress [MPa]	276.9	--	--	--
Strain [%]	-0.010277	--	--	--
Secondary failure prediction, axial stress and strain – 35 plies				
Stress [MPa]	258.9	262	262	271.1
Strain [%]	-0.010737	-0.010853	-0.010853	-0.010744
Final failure prediction, axial stress and strain - 10 plies				
Stress [MPa]	182.3	325.2	325.2	349.7
Strain [%]	0.01037	-0.014556	-0.014556	-0.014556

*Optimistic result